AIAA xxx

Spacecraft Dynamics Integrating Hinged Solar Panels and Lumped-Mass Fuel Slosh Model

Cody Allard, Manuel Diaz Ramos and Hanspeter Schaub

University of Colorado, Boulder, Colorado, 80309, US

AIAA/AAS Astrodynamics Specialist Conference
September 12–15, 2016 / Long Beach, CA

Spacecraft Dynamics Integrating Hinged Solar Panels and Lumped-Mass Fuel Slosh Model

Cody Allard,[*] Manuel Diaz Ramos[†] and Hanspeter Schaub[‡]
University of Colorado, Boulder, Colorado, 80309, US

A large portion of spacecraft missions have stringent pointing, attitude knowledge, and control requirements. This results in the necessity of high fidelity dynamics modeled in the numerical simulation of the spacecraft. A crucial aspect of this high fidelity is modeling the components susceptible to flexing and vibration. For most spacecraft, the flexible components are appended objects like solar panels and the vibrational component is fuel slosh. However, to incorporate these effects into numerical simulation, extensive derivation is required because the single rigid-body assumption no longer applies. There is significant on-going research on how to effectively model structural flexing and slosh dynamics using multi-body dynamics. However, many formulations require complex re-derivations for a specific spacecraft design. This paper introduces a ready-to-be-applied solution to rigorously integrate structural flexing and fuel slosh dynamics into a numerical simulation using the classical Newtonian and Eulerian approach. This solution can be applied to a wide variety of spacecraft configurations. This formulation approximates solar panel flexing with hinged rigid body dynamics and fuel slosh with a lumped mass vibrational model. A novel contribution of this paper is a generalized back-substitution method which can increase the computational efficiency (as much as a 180% speedup). Numerical simulations are included to show the effect of flex and slosh and the simulation is validated studying energy and momentum.

I Introduction

Flexing appended bodies and fuel slosh are the sources of excitation of vibration for many spacecraft. This vibration impacts both the translational and rotational spacecraft motion. In order to analyze these effects, it is desirable to incorporate the dynamics in fast computer simulations. However, developing the associated equations of motion (EOMs) is not a trivial task for general three-dimensional motion and often requires a custom re-derivation of the EOMs which can be time intensive. There is a need to introduce EOMs that would be applicable to many spacecraft configurations and could be used without the need of re-derivation. The EOMs considered in this paper are the translational rotational dynamics of a spacecraft with flexible structural sub-components and a tank with sloshing fuel dynamics.

There are many different ways to model flexible dynamics.[1] One method is to assume that the primary impact is on the attitude dynamics of the spacecraft so the translational motion coupling can be ignored. Also, in some scenarios the effects of flexing can be assumed to only impact one plane of rotation, therefore one method is to constrain the motion to fixed-axis rotational motion.[2] This approach allows the flexing body to be modeled as a finite number of masses on a cantilevered beam and allows for different frequency modes to be present.[2] This derivation results in a transfer function that is useful in determining the stability and frequency response due to different inputs. However, it neglects the cross coupling effect on the other rotational axes and on translational motion which does not allow for complex three-dimensional motion. This method is helpful in the early stages of a mission, but lacks fidelity and is limited in its application.

In contrast, the field of multi-body dynamics has extensive research on modeling flexible dynamics and the equations of motion presented are generalized for complex and diverse problems. This results in requiring a custom derivation of equations because of generality.[3–5] These methods are required for unique and complex systems because

[*]Graduate Student, Aerospace Engineering Sciences, University of Colorado Boulder, AIAA Student Member.
[†]Graduate Student, Aerospace Engineering Sciences, University of Colorado Boulder, AIAA Student Member..
[‡]Alfred T. and Betty E. Look Professor of Engineering, Department of Aerospace Engineering Sciences, University of Colorado, 431 UCB, Colorado Center for Astrodynamics Research, Boulder, CO 80309-0431. AIAA Associate Fellow.

the equations of motion depend on how many joints are interconnected. For example, in robotic systems, the number of interconnected joints varies widely, and the equations of motion are specific to each system.[6,7]

Similar to this paper, multiple publications present models of spacecraft dynamics with appended solar panels.[8–10] However, this previous research is mainly focused on the deployment of solar panels and how the dynamics of the spacecraft are affected.[8–10] Also, the previous research on deployable solar panels is specific to solar panels that are composed of interconnected bodies. This paper considers systems where the solar panels are single rigid bodies. It uses a method of modeling the flexible dynamics of the solar panels by assuming that the hub of the spacecraft and the solar panels are rigid bodies, but the solar panels are connected to the hub by single degree-of-freedom torsional springs.[1] The torsional spring constants could be attenuated to match the natural frequencies of the solar panels which could be found from Finite Element Analysis (FEA) or testing. This method in modeling the flexible dynamics is a first order model, and other effects like bending and torsional bending are not included.

The other vibrational driver being considered is fuel slosh. Slosh occurs when there is relative motion between a tank and the liquid it contains. The main structure of a spacecraft and the liquid exchange linear momentum, angular momentum, and energy.[11] Mathematically, the equations of motion of the structure and the liquid are tightly coupled.[12,13] In space, the liquid is subjected not only to inertial forces, but also to microgravity, viscous, and surface tension forces.[14,15] Furthermore, a moving liquid inside a tank produces a change in the position of the center of mass of the whole system in addition to internal torques and forces when a liquid wave hits the walls of the tank.

The most rigorous mathematical approach to sloshing phenomena is given by the Navier-Stokes equations with nonlinear boundary conditions.[11] Several Computational Fluid Dynamics (CFD) methods have been applied to solve this problem using different formulations.[12,13,16–18] Quasi-simultaneous methods can be used to solve the coupled equations of motion.[12] From a control perspective, however, as pointing and maneuvering requirements tighten, slosh models are needed on spacecraft with large fuel tanks to evaluate the effect of the liquid movement on the attitude control loop. The combined CFD-rigid-body model, although more exact, has some drawbacks from a simulation point of view. First, the inherent complexity of the combined model might not be feasible in early stages of the design. Second, integrating continuum and lumped models can be computationally time consuming.[19,20]

To avoid these complications, often simplified slosh models are used for control loop modeling.[14,15,21,22] Slosh is comprised of several different kinds of movement, many of which are highly nonlinear. Small-amplitude waves and stable nonlinear rotary slosh can be approximated using lumped mechanical multi-mode models,[14,15,23] including either masses, springs, and dampers or pendulums. Using a lumped model may be a useful simplification in a dynamic model for control design purposes. It can be viewed as a complement of the more accurate CFD approach. In this work, a systematic approach to slosh modeling is proposed using approximated multi-mode mechanical models. The slosh model is integrated into the rigid spacecraft and hinged panel models, providing a fully-coupled model that satisfies momentum and energy conservations. The estimation of the parameters of the model, which may be either computed through CFD simulation or observed experimentally,[19] is not considered.

Another key challenge, beyond the derivation, is the ability to create a fast numerical simulation. If the EOMs are formulated in a way where all the modes are fully cross-coupled, a large system mass matrix must be inverted which is computationally expensive. In Reference 1 a solution to decrease the computational impact for a rigid body spacecraft configuration with N hinged panel models is introduced. The resulting system mass matrix needed to be inverted for this problem is an $(N+6)\times(N+6)$ matrix. Fast computational speed is achieved by analytically back-substituting the flexing EOM into the rigid body EOM (requires an $N \times N$ inverse), and obtaining a closed form solution for the inertial angular acceleration that can be computed with the typical 3×3 matrix inverse. The flexing modes are then solved as a second stage using the found body angular acceleration term. Using this back-substitution approach, a key contribution of this paper is how to generalize this back-substitution approach for flexible dynamics and fuel slosh together.

The paper is outlined as follows. First, the nonlinearly coupled EOMs for the rigid body translational and rotational degrees of freedom are developed, followed by the EOM of the hinged panels and the fuel slosh. Next, an analytical back-substitution is presented which helps speed up the numerical evaluation. Lastly, computational performance and validation of the EOMs through energy and momentum checks is illustrated with numerical simulation of the EOMs.

II Problem Statement

The formulation assumes that there is a rigid hub, with N_S solar panels (or appended rigid bodies) and N_P lumped masses in the tank for the fuel. Subscript i is used to indicated the i_{th} solar panel and subscript j is used to indicate the j_{th} fuel slosh mass, m_j. Figure 1 displays the frame and variable definitions used for this formulation.

There are four coordinate frames defined for this formulation. The inertial reference frame is indicated by $\mathcal{N}$:

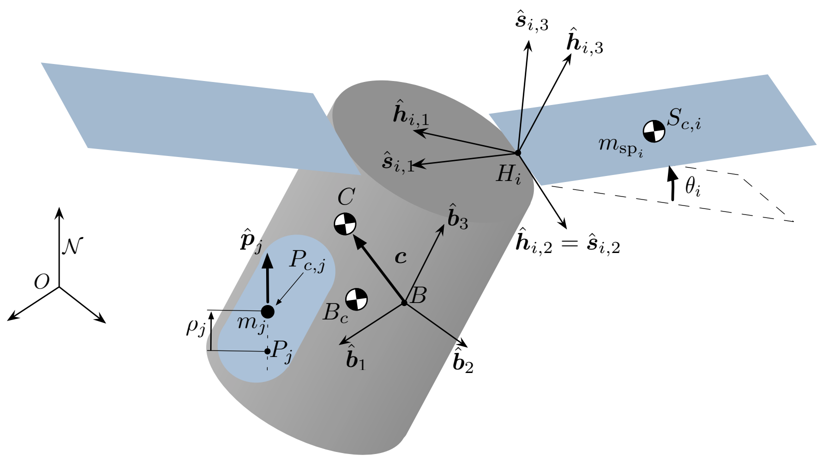

Figure 1: Frame and variable definitions used for formulation

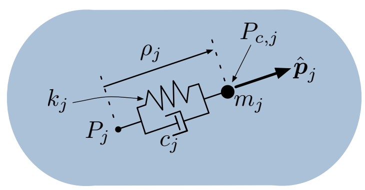

a) Detailed description of single slosh particle

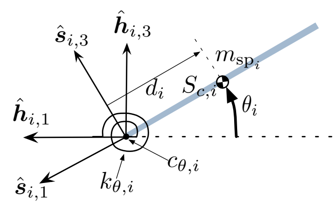

b) Detailed description of single solar panel

Figure 2: Further detail of solar panels and fuel slosh

$\{\hat{\boldsymbol{n}}_1, \hat{\boldsymbol{n}}_2, \hat{\boldsymbol{n}}_3\}$. The body fixed coordinate frame, $\mathcal{B} : \{\hat{\boldsymbol{b}}_1, \hat{\boldsymbol{b}}_2, \hat{\boldsymbol{b}}_3\}$, which is anchored to the hub and can be oriented in any direction. The solar panel frame, $\mathcal{S}_i : \{\hat{\boldsymbol{s}}_{i,1}, \hat{\boldsymbol{s}}_{i,2}, \hat{\boldsymbol{s}}_{i,3}\}$, is a frame with its origin located at its corresponding hinge location, H_i. The $\mathcal{S}_i$ frame is oriented such that $\hat{\boldsymbol{s}}_{i,1}$ points antiparallel to the center of mass of its solar panel, $S_{c,i}$. The $\hat{\boldsymbol{s}}_{i,2}$ axis is defined as the rotation axis that would yield a positive θ_i using the right-hand rule. The distance from point H_i to point $S_{c,i}$ is defined as d_i. The hinge frame, $\mathcal{H}_i : \{\hat{\boldsymbol{h}}_{i,1}, \hat{\boldsymbol{h}}_{i,2}, \hat{\boldsymbol{h}}_{i,3}\}$, is a frame fixed with respect to the body frame, and is equivalent to the respective $\mathcal{S}_i$ frame when the corresponding solar panel is undeflected.

There are a few more key locations that need to be defined. Point B is the origin of the body frame, and can have any location with respect to the hub. Point B_c is the location of the center of mass of the rigid hub. P_j is the undeflected or equilibrium position of each corresponding slosh mass, while point $P_{c,j}$ is the current position of that slosh mass.

Figure 2 provides further detail of the fuel slosh and hinged solar panel parameters. As seen in Figure 2(a), an individual slosh particle is constrained to move along its corresponding $\hat{\boldsymbol{p}}_j$ direction while connected by a spring with a linear spring constant value k_j and by a linear damper with a damping coefficient, c_j. The variable, ρ_j is a state variable and quantifies the displacement from equilibrium for the corresponding slosh mass. Analogously, Figure 2(b) shows that each solar panel, with mass m_{sp_i}, is connected by a torsional spring with spring constant, $k_{\theta,i}$ and has a rotational damper with coefficient $c_{\theta,i}$. The state variable describing a solar panel's angular displacement from equilibrium is θ_i.

Using the variables and frames defined, the following section outlines the derivation of equations of motion for the spacecraft.

III Derivation of Equations of Motion

III.A Rigid Spacecraft Hub Translational Motion

Following a similar derivation as in previous work,[1] the derivation begins with Newton's first law for the center of mass of the spacecraft.

$$\ddot{\boldsymbol{r}}_{C/N} = \frac{\boldsymbol{F}}{m_{\text{sc}}} \tag{1}$$

Ultimately the acceleration of the body frame or point B is desired

$$\ddot{\boldsymbol{r}}_{B/N} = \ddot{\boldsymbol{r}}_{C/N} - \ddot{\boldsymbol{c}} \tag{2}$$

The definition of $\boldsymbol{c}$ can be seen in Eq. (3).

$$\boldsymbol{c} = \frac{1}{m_{\text{sc}}}\Big(m_{\text{hub}}\boldsymbol{r}_{B_c/B} + \sum_{i=1}^{N_S} m_{\text{sp}_i}\boldsymbol{r}_{S_{c,i}/B} + \sum_{j=1}^{N_P} m_j \boldsymbol{r}_{P_{c,j}/B}\Big) \tag{3}$$

To find the inertial time derivative of $\boldsymbol{c}$, it is first necessary to find the time derivative of $\boldsymbol{c}$ with respect to the body frame. A time derivative of any vector, $\boldsymbol{v}$, with respect to the body frame is denoted by $\boldsymbol{v}'$; the inertial time derivative is labeled as $\dot{\boldsymbol{v}}$. The first and second body-relative time derivatives of $\boldsymbol{c}$ can be seen in Eqs. (4) and (5).

$$\boldsymbol{c}' = \frac{1}{m_{\text{sc}}}\Big(\sum_{i=1}^{N_S} m_{\text{sp}_i}\boldsymbol{r}'_{S_{c,i}/B} + \sum_{j=1}^{N_P} m_j \boldsymbol{r}'_{P_{c,j}/B}\Big) \tag{4}$$

$$\boldsymbol{c}'' = \frac{1}{m_{\text{sc}}}\Big(\sum_{i=1}^{N_S} m_{\text{sp}_i}\boldsymbol{r}''_{S_{c,i}/B} + \sum_{j=1}^{N_P} m_j \boldsymbol{r}''_{P_{c,j}/B}\Big) \tag{5}$$

The vector $\boldsymbol{r}_{S_{c,i}/B}$ is readily defined using the $\hat{\boldsymbol{s}}_{i,1}$ axis

$$\boldsymbol{r}_{S_{c,i}/B} = \boldsymbol{r}_{H_i/B} - d_i\hat{\boldsymbol{s}}_{i,1} \tag{6}$$

Now the first and second time derivatives with respect to the body frame of $\boldsymbol{r}_{S_{c,i}/B}$ are taken

$$\boldsymbol{r}'_{S_{c,i}/B} = d_i\dot{\theta}_i\hat{\boldsymbol{s}}_{i,3} \tag{7}$$

$$\boldsymbol{r}''_{S_{c,i}/B} = d_i\left(\ddot{\theta}_i\hat{\boldsymbol{s}}_{i,3} + \dot{\theta}_i^2\hat{\boldsymbol{s}}_{i,1}\right) \tag{8}$$

Similarly $\boldsymbol{r}_{P_{c,j}/B}$ is defined in the following

$$\boldsymbol{r}_{P_{c,j}/B} = \boldsymbol{r}_{P_j/B} + \rho_j\hat{\boldsymbol{p}}_j \tag{9}$$

And, the first and second body time derivatives of $\boldsymbol{r}_{P_{c,j}/B}$ are

$$\boldsymbol{r}'_{P_{c,j}/B} = \dot{\rho}_j\hat{\boldsymbol{p}}_j \tag{10}$$

$$\boldsymbol{r}''_{P_{c,j}/B} = \ddot{\rho}_j\hat{\boldsymbol{p}}_j \tag{11}$$

Eqs. (4) and (5) are next reformulated to include these new definitions:

$$\boldsymbol{c}' = \frac{1}{m_{\text{sc}}}\Big(\sum_{i=1}^{N_S} m_{\text{sp}_i}d_i\dot{\theta}_i\hat{\boldsymbol{s}}_{i,3} + \sum_{j=1}^{N_P} m_j\dot{\rho}_j\hat{\boldsymbol{p}}_j\Big) \tag{12}$$

$$\boldsymbol{c}'' = \frac{1}{m_{\text{sc}}}\Big[\sum_{i=1}^{N_S} m_{\text{sp}_i}d_i\left(\ddot{\theta}_i\hat{\boldsymbol{s}}_{i,3} + \dot{\theta}_i^2\hat{\boldsymbol{s}}_{i,1}\right) + \sum_{j=1}^{N_P} m_j\ddot{\rho}_j\hat{\boldsymbol{p}}_j\Big] \tag{13}$$

Using the transport theorem[24] yields the following definition for $\ddot{\boldsymbol{c}}$

$$\ddot{\boldsymbol{c}} = \boldsymbol{c}'' + 2\boldsymbol{\omega}_{\mathcal{B}/\mathcal{N}} \times \boldsymbol{c}' + \dot{\boldsymbol{\omega}}_{\mathcal{B}/\mathcal{N}} \times \boldsymbol{c} + \boldsymbol{\omega}_{\mathcal{B}/\mathcal{N}} \times \left(\boldsymbol{\omega}_{\mathcal{B}/\mathcal{N}} \times \boldsymbol{c}\right) \tag{14}$$

Eq. (2) is updated to include Eq. (14)

$$\ddot{\boldsymbol{r}}_{B/N} = \ddot{\boldsymbol{r}}_{C/N} - \boldsymbol{c}'' - 2\boldsymbol{\omega}_{\mathcal{B}/\mathcal{N}} \times \boldsymbol{c}' - \dot{\boldsymbol{\omega}}_{\mathcal{B}/\mathcal{N}} \times \boldsymbol{c} - \boldsymbol{\omega}_{\mathcal{B}/\mathcal{N}} \times \left(\boldsymbol{\omega}_{\mathcal{B}/\mathcal{N}} \times \boldsymbol{c}\right) \tag{15}$$

Substituting Eq.(13) into Eq.(15) results in

$$\ddot{\boldsymbol{r}}_{B/N} = \ddot{\boldsymbol{r}}_{C/N} - \frac{1}{m_{\text{sc}}}\left[\sum_{i=1}^{N_S} m_{\text{sp}_i} d_i \left(\ddot{\theta}_i \hat{\boldsymbol{s}}_{i,3} + \dot{\theta}_i^2 \hat{\boldsymbol{s}}_{i,1}\right) + \sum_{j=1}^{N_P} m_j \ddot{\rho}_j \hat{\boldsymbol{p}}_j\right] - 2\boldsymbol{\omega}_{\mathcal{B}/\mathcal{N}} \times \boldsymbol{c}' - \dot{\boldsymbol{\omega}}_{\mathcal{B}/\mathcal{N}} \times \boldsymbol{c} - \boldsymbol{\omega}_{\mathcal{B}/\mathcal{N}} \times \left(\boldsymbol{\omega}_{\mathcal{B}/\mathcal{N}} \times \boldsymbol{c}\right) \tag{16}$$

Moving second order terms to the left hand side and introducing the tilde matrix[24] to replace the cross product operators simplifies the equation to

$$\ddot{\boldsymbol{r}}_{B/N} - [\tilde{\boldsymbol{c}}]\dot{\boldsymbol{\omega}}_{\mathcal{B}/\mathcal{N}} + \frac{1}{m_{\text{sc}}}\sum_{i=1}^{N_S} m_{\text{sp}_i} d_i \hat{\boldsymbol{s}}_{i,3}\ddot{\theta}_i + \frac{1}{m_{\text{sc}}}\sum_{j=1}^{N_P} m_j \hat{\boldsymbol{p}}_j \ddot{\rho}_j = \ddot{\boldsymbol{r}}_{C/N} - 2[\tilde{\boldsymbol{\omega}}_{\mathcal{B}/\mathcal{N}}]\boldsymbol{c}' - [\tilde{\boldsymbol{\omega}}_{\mathcal{B}/\mathcal{N}}][\tilde{\boldsymbol{\omega}}_{\mathcal{B}/\mathcal{N}}]\boldsymbol{c} - \frac{1}{m_{\text{sc}}}\sum_{i=1}^{N_S} m_{\text{sp}_i} d_i \dot{\theta}_i^2 \hat{\boldsymbol{s}}_{i,1} \tag{17}$$

Equation (17) is the translational motion equation and is the first EOM needed to describe the motion of the spacecraft. The following section develops the rotational EOM.

III.B Rigid Spacecraft Hub Rotational Motion

Starting with Euler's equation when the body fixed coordinate frame origin is not coincident with the center of mass of the body[24]

$$\dot{\boldsymbol{H}}_{\text{sc},B} = \boldsymbol{L}_B + m_{\text{sc}}\ddot{\boldsymbol{r}}_{B/N} \times \boldsymbol{c} \tag{18}$$

where $\boldsymbol{L}_B$ is the total external torque about point B. The definition of the angular momentum vector of the spacecraft about point B is

$$\boldsymbol{H}_{\text{sc},B} = [I_{\text{hub},B_c}]\boldsymbol{\omega}_{\mathcal{B}/\mathcal{N}} + m_{\text{hub}}\boldsymbol{r}_{B_c/B} \times \dot{\boldsymbol{r}}_{B_c/B} + \sum_{j=1}^{N_P} m_j \boldsymbol{r}_{P_{c,j}/B} \times \dot{\boldsymbol{r}}_{P_{c,j}/B} + \sum_{i=1}^{N_S}\left([I_{\text{sp}_i,S_{c,i}}]\boldsymbol{\omega}_{\mathcal{B}/\mathcal{N}} + \dot{\theta}_i I_{s_{i,2}}\hat{\boldsymbol{s}}_{i,2} + m_{\text{sp}_i}\boldsymbol{r}_{S_{c,i}/B} \times \dot{\boldsymbol{r}}_{S_{c,i}/B}\right) \tag{19}$$

The solar panel inertia about its center of mass is assumed to be defined along principal inertia axes and is of the form

$$[I_{\text{sp}_i,S_{c,i}}] = {}^{\mathcal{S}}\begin{bmatrix} I_{s_{i,1}} & 0 & 0 \\ 0 & I_{s_{i,2}} & 0 \\ 0 & 0 & I_{s_{i,3}} \end{bmatrix} \tag{20}$$

Now the inertial time derivative of Eq. (19) is taken and yields

$$\begin{aligned}\dot{\boldsymbol{H}}_{\text{sc},B} = {} & [I_{\text{hub},B_c}]\dot{\boldsymbol{\omega}}_{\mathcal{B}/\mathcal{N}} + \boldsymbol{\omega}_{\mathcal{B}/\mathcal{N}} \times [I_{\text{hub},B_c}]\boldsymbol{\omega}_{\mathcal{B}/\mathcal{N}} + m_{\text{hub}}\boldsymbol{r}_{B_c/B} \times \ddot{\boldsymbol{r}}_{B_c/B} + \sum_{j=1}^{N_P} m_j \boldsymbol{r}_{P_{c,j}/B} \times \ddot{\boldsymbol{r}}_{P_{c,j}/B} \\ & + \sum_{i=1}^{N_S}\Big([I'_{\text{sp}_i,S_{c,i}}]\boldsymbol{\omega}_{\mathcal{B}/\mathcal{N}} + [I_{\text{sp}_i,S_{c,i}}]\dot{\boldsymbol{\omega}}_{\mathcal{B}/\mathcal{N}} + \boldsymbol{\omega}_{\mathcal{B}/\mathcal{N}} \times [I_{\text{sp}_i,S_{c,i}}]\boldsymbol{\omega}_{\mathcal{B}/\mathcal{N}} \\ & + \ddot{\theta}_i I_{s_{i,2}}\hat{\boldsymbol{s}}_{i,2} + \boldsymbol{\omega}_{\mathcal{B}/\mathcal{N}} \times \dot{\theta}_i I_{s_{i,2}}\hat{\boldsymbol{s}}_{i,2} + m_{\text{sp}_i}\boldsymbol{r}_{S_{c,i}/B} \times \ddot{\boldsymbol{r}}_{S_{c,i}/B}\Big)\end{aligned} \tag{21}$$

The terms $\ddot{\boldsymbol{r}}_{B_c/B}$, $\ddot{\boldsymbol{r}}_{S_{c,i}/B}$ and $\ddot{\boldsymbol{r}}_{P_{c,j}/B}$ are found using the transport theorem and knowing that $\boldsymbol{r}_{B_c/B}$ is fixed with respect to the body frame.

$$\ddot{\boldsymbol{r}}_{B_c/B} = \dot{\boldsymbol{\omega}}_{\mathcal{B}/\mathcal{N}} \times \boldsymbol{r}_{B_c/B} + \boldsymbol{\omega}_{\mathcal{B}/\mathcal{N}} \times (\boldsymbol{\omega}_{\mathcal{B}/\mathcal{N}} \times \boldsymbol{r}_{B_c/B}) \tag{22}$$

$$\ddot{\boldsymbol{r}}_{S_{c,i}/B} = \boldsymbol{r}''_{S_{c,i}/B} + 2\boldsymbol{\omega}_{\mathcal{B}/\mathcal{N}} \times \boldsymbol{r}'_{S_{c,i}/B} + \dot{\boldsymbol{\omega}}_{\mathcal{B}/\mathcal{N}} \times \boldsymbol{r}_{S_{c,i}/B} + \boldsymbol{\omega}_{\mathcal{B}/\mathcal{N}} \times (\boldsymbol{\omega}_{\mathcal{B}/\mathcal{N}} \times \boldsymbol{r}_{S_{c,i}/B}) \tag{23}$$

$$\ddot{\boldsymbol{r}}_{P_{c,j}/B} = \boldsymbol{r}''_{P_{c,j}/B} + 2\boldsymbol{\omega}_{\mathcal{B}/\mathcal{N}} \times \boldsymbol{r}'_{P_{c,j}/B} + \dot{\boldsymbol{\omega}}_{\mathcal{B}/\mathcal{N}} \times \boldsymbol{r}_{P_{c,j}/B} + \boldsymbol{\omega}_{\mathcal{B}/\mathcal{N}} \times (\boldsymbol{\omega}_{\mathcal{B}/\mathcal{N}} \times \boldsymbol{r}_{P_{c,j}/B}) \tag{24}$$

Incorporating Eqs. (22) - (24) into Eq. (21) results in

$$\begin{aligned}\dot{\boldsymbol{H}}_{\text{sc},B} &= [I_{\text{hub},B_c}]\dot{\boldsymbol{\omega}}_{\mathcal{B}/\mathcal{N}} + \boldsymbol{\omega}_{\mathcal{B}/\mathcal{N}} \times [I_{\text{hub},B_c}]\boldsymbol{\omega}_{\mathcal{B}/\mathcal{N}} + m_{\text{hub}}\boldsymbol{r}_{B_c/B} \times (\dot{\boldsymbol{\omega}}_{\mathcal{B}/\mathcal{N}} \times \boldsymbol{r}_{B_c/B}) \\
&+ m_{\text{hub}}\boldsymbol{r}_{B_c/B} \times \Big[\boldsymbol{\omega}_{\mathcal{B}/\mathcal{N}} \times (\boldsymbol{\omega}_{\mathcal{B}/\mathcal{N}} \times \boldsymbol{r}_{B_c/B})\Big] + \sum_{j=1}^{N_P} m_j \boldsymbol{r}_{P_{c,j}/B} \times \Big[\boldsymbol{r}''_{P_{c,j}/B} + 2\boldsymbol{\omega}_{\mathcal{B}/\mathcal{N}} \times \boldsymbol{r}'_{P_{c,j}/B} + \dot{\boldsymbol{\omega}}_{\mathcal{B}/\mathcal{N}} \times \boldsymbol{r}_{P_{c,j}/B} \\
&+ \boldsymbol{\omega}_{\mathcal{B}/\mathcal{N}} \times (\boldsymbol{\omega}_{\mathcal{B}/\mathcal{N}} \times \boldsymbol{r}_{P_{c,j}/B})\Big] + \sum_{i=1}^{N_S}\Big([I'_{\text{sp}_i,S_{c,i}}]\boldsymbol{\omega}_{\mathcal{B}/\mathcal{N}} + [I_{\text{sp}_i,S_{c,i}}]\dot{\boldsymbol{\omega}}_{\mathcal{B}/\mathcal{N}} + \boldsymbol{\omega}_{\mathcal{B}/\mathcal{N}} \times [I_{\text{sp}_i,S_{c,i}}]\boldsymbol{\omega}_{\mathcal{B}/\mathcal{N}} \\
&+ \ddot{\theta}_i I_{s_{i,2}}\hat{\boldsymbol{s}}_{i,2} + \boldsymbol{\omega}_{\mathcal{B}/\mathcal{N}} \times \dot{\theta}_i I_{s_{i,2}}\hat{\boldsymbol{s}}_{i,2} + m_{\text{sp}_i}\boldsymbol{r}_{S_{c,i}/B} \times \boldsymbol{r}''_{S_{c,i}/B} + 2m_{\text{sp}_i}\boldsymbol{r}_{S_{c,i}/B} \times (\boldsymbol{\omega}_{\mathcal{B}/\mathcal{N}} \times \boldsymbol{r}'_{S_{c,i}/B}) \\
&+ m_{\text{sp}_i}\boldsymbol{r}_{S_{c,i}/B} \times (\dot{\boldsymbol{\omega}}_{\mathcal{B}/\mathcal{N}} \times \boldsymbol{r}_{S_{c,i}/B}) + m_{\text{sp}_i}\boldsymbol{r}_{S_{c,i}/B} \times [\boldsymbol{\omega}_{\mathcal{B}/\mathcal{N}} \times (\boldsymbol{\omega}_{\mathcal{B}/\mathcal{N}} \times \boldsymbol{r}_{S_{c,i}/B})]\Big) \end{aligned} \tag{25}$$

Applying the parallel axis theorem the following inertia tensor terms are defined as

$$[I_{\text{hub},B}] = [I_{\text{hub},B_c}] + m_{\text{hub}}[\tilde{\boldsymbol{r}}_{B_c/B}][\tilde{\boldsymbol{r}}_{B_c/B}]^T \tag{26}$$

$$[I_{\text{sp}_i,B}] = [I_{\text{sp}_i,S_{c,i}}] + m_{\text{sp}_i}[\tilde{\boldsymbol{r}}_{S_{c,i}/B}][\tilde{\boldsymbol{r}}_{S_{c,i}/B}]^T \tag{27}$$

$$[I_{\text{sc},B}] = [I_{\text{hub},B}] + \sum_{i=1}^{N_S}[I_{\text{sp}_i,B}] + \sum_{j=1}^{N_P} m_j[\tilde{\boldsymbol{r}}_{P_{c,j}/B}][\tilde{\boldsymbol{r}}_{P_{c,j}/B}]^T \tag{28}$$

Taking the body-relative time derivative of Equation (28) yields

$$\begin{aligned}[I'_{\text{sc},B}] &= \sum_{i=1}^{N_S}\Big[[I'_{\text{sp}_i,S_{c,i}}] - m_{\text{sp}_i}\Big([\tilde{\boldsymbol{r}}'_{S_{c,i}/B}][\tilde{\boldsymbol{r}}_{S_{c,i}/B}] + [\tilde{\boldsymbol{r}}_{S_{c,i}/B}][\tilde{\boldsymbol{r}}'_{S_{c,i}/B}]\Big)\Big] \\
&- \sum_{j=1}^{N_P} m_j\Big([\tilde{\boldsymbol{r}}'_{P_{c,j}/B}][\tilde{\boldsymbol{r}}_{P_{c,j}/B}] + [\tilde{\boldsymbol{r}}_{P_{c,j}/B}][\tilde{\boldsymbol{r}}'_{P_{c,j}/B}]\Big)\end{aligned} \tag{29}$$

$[I'_{\text{sp}_i,S_{c,i}}]$ needs to be defined and can be conveniently expressed by leveraging the assumption that the inertia matrix is diagonal and is written in terms of its base vectors:

$$[I_{\text{sp}_i,S_{c,i}}] = I_{s_{i,1}}\hat{\boldsymbol{s}}_{i,1}\hat{\boldsymbol{s}}_{i,1}^T + I_{s_{i,2}}\hat{\boldsymbol{s}}_{i,2}\hat{\boldsymbol{s}}_{i,2}^T + I_{s_{i,3}}\hat{\boldsymbol{s}}_{i,3}\hat{\boldsymbol{s}}_{i,3}^T \tag{30}$$

Taking the body time derivative of Eq. (30) results in

$$[I'_{\text{sp}_i,S_{c,i}}] = I_{s_{i,1}}\hat{\boldsymbol{s}}'_{i,1}\hat{\boldsymbol{s}}_{i,1}^T + I_{s_{i,1}}\hat{\boldsymbol{s}}_{i,1}\hat{\boldsymbol{s}}_{i,1}'^T + I_{s_{i,2}}\hat{\boldsymbol{s}}'_{i,2}\hat{\boldsymbol{s}}_{i,2}^T + I_{s_{i,2}}\hat{\boldsymbol{s}}_{i,2}\hat{\boldsymbol{s}}_{i,2}'^T + I_{s_{i,3}}\hat{\boldsymbol{s}}'_{i,3}\hat{\boldsymbol{s}}_{i,3}^T + I_{s_{i,3}}\hat{\boldsymbol{s}}_{i,3}\hat{\boldsymbol{s}}_{i,3}'^T \tag{31}$$

Using the transport theorem: $\hat{\boldsymbol{s}}'_{i,j} = \boldsymbol{\omega}_{\mathcal{S}_i/\mathcal{B}} \times \hat{\boldsymbol{s}}_{i,j} = \dot{\theta}_i\hat{\boldsymbol{s}}_{i,2} \times \hat{\boldsymbol{s}}_{i,j}$, and applying this to Eq. (31) and simplifying results in

$$[I'_{\text{sp}_i,S_{c,i}}] = \dot{\theta}_i(I_{s_{i,3}} - I_{s_{i,1}})(\hat{\boldsymbol{s}}_{i,1}\hat{\boldsymbol{s}}_{i,3}^T + \hat{\boldsymbol{s}}_{i,3}\hat{\boldsymbol{s}}_{i,1}^T) \tag{32}$$

Substituting Eq. (32) into Eq. (25) and using Eq. (28) to simplify results in Eq. (33). The Jacobi Identity, $(\boldsymbol{a} \times \boldsymbol{b}) \times \boldsymbol{c} = \boldsymbol{a} \times (\boldsymbol{b} \times \boldsymbol{c}) - \boldsymbol{b} \times (\boldsymbol{a} \times \boldsymbol{c})$, is used to combine terms and produce the following simplified equation

$$\begin{aligned}\dot{\boldsymbol{H}}_{\text{sc},B} &= [I_{\text{sc},B}]\dot{\boldsymbol{\omega}}_{\mathcal{B}/\mathcal{N}} + \boldsymbol{\omega}_{\mathcal{B}/\mathcal{N}} \times [I_{\text{sc},B}]\boldsymbol{\omega}_{\mathcal{B}/\mathcal{N}} + [I'_{\text{sc},B}]\boldsymbol{\omega}_{\mathcal{B}/\mathcal{N}} + \sum_{j=1}^{N_P}\Big[m_j\boldsymbol{r}_{P_{c,j}/B} \times \boldsymbol{r}''_{P_{c,j}/B} \\
&+ m_j\boldsymbol{\omega}_{\mathcal{B}/\mathcal{N}} \times \Big(\boldsymbol{r}_{P_{c,j}/B} \times \boldsymbol{r}'_{P_{c,j}/B}\Big)\Big] + \sum_{i=1}^{N_S}\Big[\ddot{\theta}_i I_{s_{i,2}}\hat{\boldsymbol{s}}_{i,2} + \boldsymbol{\omega}_{\mathcal{B}/\mathcal{N}} \times \dot{\theta}_i I_{s_{i,2}}\hat{\boldsymbol{s}}_{i,2} \\
&+ m_{\text{sp}_i}\boldsymbol{r}_{S_{c,i}/B} \times \boldsymbol{r}''_{S_{c,i}/B} + m_{\text{sp}_i}\boldsymbol{\omega}_{\mathcal{B}/\mathcal{N}} \times \Big(\boldsymbol{r}_{S_{c,i}/B} \times \boldsymbol{r}'_{S_{c,i}/B}\Big)\Big]\end{aligned} \tag{33}$$

Eqs. (18) and (33) are equated and yield

$$\boldsymbol{L}_B + m_{\text{sc}}\ddot{\boldsymbol{r}}_{B/N} \times \boldsymbol{c} = [I_{\text{sc},B}]\dot{\boldsymbol{\omega}}_{\mathcal{B}/\mathcal{N}} + \boldsymbol{\omega}_{\mathcal{B}/\mathcal{N}} \times [I_{\text{sc},B}]\boldsymbol{\omega}_{\mathcal{B}/\mathcal{N}} + [I'_{\text{sc},B}]\boldsymbol{\omega}_{\mathcal{B}/\mathcal{N}} + \sum_{j=1}^{N_P}\Big[m_j\boldsymbol{r}_{P_{c,j}/B} \times \boldsymbol{r}''_{P_{c,j}/B} + m_j\boldsymbol{\omega}_{\mathcal{B}/\mathcal{N}} \times \Big(\boldsymbol{r}_{P_{c,j}/B} \times \boldsymbol{r}'_{P_{c,j}/B}\Big)\Big] + \sum_{i=1}^{N_S}\Big[\ddot{\theta}_i I_{s_{i,2}}\hat{\boldsymbol{s}}_{i,2} + \boldsymbol{\omega}_{\mathcal{B}/\mathcal{N}} \times \dot{\theta}_i I_{s_{i,2}}\hat{\boldsymbol{s}}_{i,2} + m_{\text{sp}_i}\boldsymbol{r}_{S_{c,i}/B} \times \boldsymbol{r}''_{S_{c,i}/B} + m_{\text{sp}_i}\boldsymbol{\omega}_{\mathcal{B}/\mathcal{N}} \times \Big(\boldsymbol{r}_{S_{c,i}/B} \times \boldsymbol{r}'_{S_{c,i}/B}\Big)\Big] \tag{34}$$

Finally, using tilde matrix and simplifying yields the modified Euler equation, which is the second EOM necessary to describe the motion of the spacecraft.

$$[I_{\text{sc},B}]\dot{\boldsymbol{\omega}}_{\mathcal{B}/\mathcal{N}} = -[\tilde{\boldsymbol{\omega}}_{\mathcal{B}/\mathcal{N}}][I_{\text{sc},B}]\boldsymbol{\omega}_{\mathcal{B}/\mathcal{N}} - [I'_{\text{sc},B}]\boldsymbol{\omega}_{\mathcal{B}/\mathcal{N}} - \sum_{j=1}^{N_P}\Big(m_j[\tilde{\boldsymbol{r}}_{P_{c,j}/B}]\boldsymbol{r}''_{P_{c,j}/B} + m_j[\tilde{\boldsymbol{\omega}}_{\mathcal{B}/\mathcal{N}}][\tilde{\boldsymbol{r}}_{P_{c,j}/B}]\boldsymbol{r}'_{P_{c,j}/B}\Big) - \sum_{i=1}^{N_S}\Big(\ddot{\theta}_i I_{s_{i,2}}\hat{\boldsymbol{s}}_{i,2} + [\tilde{\boldsymbol{\omega}}_{\mathcal{B}/\mathcal{N}}]\dot{\theta}_i I_{s_{i,2}}\hat{\boldsymbol{s}}_{i,2} + m_{\text{sp}_i}[\tilde{\boldsymbol{r}}_{S_{c,i}/B}]\boldsymbol{r}''_{S_{c,i}/B} + m_{\text{sp}_i}[\tilde{\boldsymbol{\omega}}_{\mathcal{B}/\mathcal{N}}][\tilde{\boldsymbol{r}}_{S_{c,i}/B}]\boldsymbol{r}'_{S_{c,i}/B}\Big) + \boldsymbol{L}_B - m_{\text{sc}}[\tilde{\boldsymbol{c}}]\ddot{\boldsymbol{r}}_{B/N} \tag{35}$$

Rearranging Eq. (35) to be in the same form as the previous sections results in

$$m_{\text{sc}}[\tilde{\boldsymbol{c}}]\ddot{\boldsymbol{r}}_{B/N} + [I_{\text{sc},B}]\dot{\boldsymbol{\omega}}_{\mathcal{B}/\mathcal{N}} + \sum_{i=1}^{N_S}\Big\{I_{s_{i,2}}\hat{\boldsymbol{s}}_{i,2} + m_{\text{sp}_i}d_i[\tilde{\boldsymbol{r}}_{S_{c,i}/B}]\hat{\boldsymbol{s}}_{i,3}\Big\}\ddot{\theta}_i + \sum_{j=1}^{N_P}m_j[\tilde{\boldsymbol{r}}_{P_{c,j}/B}]\hat{\boldsymbol{p}}_j\ddot{\rho}_j = -[\tilde{\boldsymbol{\omega}}_{\mathcal{B}/\mathcal{N}}][I_{\text{sc},B}]\boldsymbol{\omega}_{\mathcal{B}/\mathcal{N}} - [I'_{\text{sc},B}]\boldsymbol{\omega}_{\mathcal{B}/\mathcal{N}} - \sum_{i=1}^{N_S}\Big\{\dot{\theta}_i[\tilde{\boldsymbol{\omega}}_{\mathcal{B}/\mathcal{N}}]\left(I_{s_{i,2}}\hat{\boldsymbol{s}}_{i,2} + m_{\text{sp}_i}d_i[\tilde{\boldsymbol{r}}_{S_{c,i}/B}]\hat{\boldsymbol{s}}_{i,3}\right) + m_{\text{sp}_i}d_i\dot{\theta}_i^2[\tilde{\boldsymbol{r}}_{S_{c,i}/B}]\hat{\boldsymbol{s}}_{i,1}\Big\} - \sum_{j=1}^{N_P}m_j[\tilde{\boldsymbol{\omega}}_{\mathcal{B}/\mathcal{N}}][\tilde{\boldsymbol{r}}_{P_{c,j}/B}]\boldsymbol{r}'_{P_{c,j}/B} + \boldsymbol{L}_B \tag{36}$$

III.C Solar Panel Motion

The following section follows the same derivation seen in previous work[1] and is summarized here for convenience. Let $\boldsymbol{L}_{H_i} = L_{i,1}\hat{\boldsymbol{s}}_{i,1} + L_{i,2}\hat{\boldsymbol{s}}_{i,2} + L_{i,3}\hat{\boldsymbol{s}}_{i,3}$ be the total torque acting on the solar panel. The corresponding hinge torque is given through

$$L_{i,2} = -k_i\theta_i - c_i\dot{\theta}_i + \hat{\boldsymbol{s}}_{i,2} \cdot \boldsymbol{\tau}_{\text{ext},H_i} \tag{37}$$

The hinge structure produces the other two torques $L_{i,1}$ and $L_{i,3}$. $\boldsymbol{\tau}_{\text{ext},H_i}$ is the external torque on the solar panel and is projected onto the $\hat{\boldsymbol{s}}_{i,2}$ direction to find its contribution to $L_{i,2}$. Gravity, for example would apply the following torque on the solar panel about point H_i

$$\boldsymbol{\tau}_{g,H_i} = \boldsymbol{r}_{S_{c,i}/H_i} \times \boldsymbol{F}_g \tag{38}$$

The inertial angular velocity vector for the solar panel frame is

$$\boldsymbol{\omega}_{\mathcal{S}_i/\mathcal{N}} = \boldsymbol{\omega}_{\mathcal{S}_i/\mathcal{H}_i} + \boldsymbol{\omega}_{\mathcal{H}_i/\mathcal{B}} + \boldsymbol{\omega}_{\mathcal{B}/\mathcal{N}} \tag{39}$$

where $\boldsymbol{\omega}_{\mathcal{S}_i/\mathcal{H}_i} = \dot{\theta}_i\hat{\boldsymbol{s}}_{i,2}$. Because the hinge frame $\mathcal{H}_i$ is fixed relative to the body frame $\mathcal{B}$ the relative angular velocity vector is $\boldsymbol{\omega}_{\mathcal{H}_i/\mathcal{B}} = \boldsymbol{0}$. The body angular velocity vector is written in $\mathcal{S}_i$-frame components as

$$\boldsymbol{\omega}_{\mathcal{B}/\mathcal{N}} = (\hat{\boldsymbol{s}}_{i,1} \cdot \boldsymbol{\omega}_{\mathcal{B}/\mathcal{N}})\hat{\boldsymbol{s}}_{i,1} + (\hat{\boldsymbol{s}}_{i,2} \cdot \boldsymbol{\omega}_{\mathcal{B}/\mathcal{N}})\hat{\boldsymbol{s}}_{i,2} + (\hat{\boldsymbol{s}}_{i,3} \cdot \boldsymbol{\omega}_{\mathcal{B}/\mathcal{N}})\hat{\boldsymbol{s}}_{i,3} \tag{40}$$

$$= \omega_{s_{i,1}}\hat{\boldsymbol{s}}_{i,1} + \omega_{s_{i,2}}\hat{\boldsymbol{s}}_{i,2} + \omega_{s_{i,3}}\hat{\boldsymbol{s}}_{i,3} \tag{41}$$

Using this definition greatly simplifies the following algebraic development. Finally, the inertial solar panel angular velocity vector is written as

$$\boldsymbol{\omega}_{\mathcal{S}_i/\mathcal{N}} = \omega_{s_{i,1}}\hat{\boldsymbol{s}}_{i,1} + (\omega_{s_{i,2}} + \dot{\theta}_i)\hat{\boldsymbol{s}}_{i,2} + \omega_{s_{i,3}}\hat{\boldsymbol{s}}_{i,3} \tag{42}$$

As $\hat{\boldsymbol{s}}_{i,2}$ is a body-fixed vector, note that

$$\dot{\omega}_{s_{i,2}} = \frac{{}^{\mathcal{B}}\mathrm{d}}{\mathrm{d}t}\left(\boldsymbol{\omega}_{\mathcal{B}/\mathcal{N}} \cdot \hat{\boldsymbol{s}}_{i,2}\right) = \frac{{}^{\mathcal{B}}\mathrm{d}}{\mathrm{d}t}\left(\boldsymbol{\omega}_{\mathcal{B}/\mathcal{N}}\right) \cdot \hat{\boldsymbol{s}}_{i,2} = \dot{\boldsymbol{\omega}}_{\mathcal{B}/\mathcal{N}} \cdot \hat{\boldsymbol{s}}_{i,2} \tag{43}$$

Substituting these angular velocity components into the rotational equations of motion of a rigid body with torques taken about its center of mass,[24] the general solar panel equations of motion are written as

$$I_{s_{i,1}}\dot{\omega}_{s_{i,1}} = -(I_{s_{i,3}} - I_{s_{i,2}})(\omega_{s_{i,2}} + \dot{\theta}_i)\omega_{s_{i,3}} + L_{s_{i,1}} \tag{44}$$

$$I_{s_{i,2}}(\dot{\omega}_{s_{i,2}} + \ddot{\theta}_i) = -(I_{s_{i,1}} - I_{s_{i,3}})\omega_{s_{i,3}}\omega_{s_{i,1}} + L_{s_{i,2}} \tag{45}$$

$$I_{s_{i,3}}\dot{\omega}_{s_{i,3}} = -(I_{s_{i,2}} - I_{s_{i,1}})\omega_{s_{i,1}}(\omega_{s_{i,2}} + \dot{\theta}_i) + L_{s_{i,3}} \tag{46}$$

where $\boldsymbol{L}_{S_{c,i}} = L_{s_{i,1}}\hat{\boldsymbol{s}}_{i,1} + L_{s_{i,2}}\hat{\boldsymbol{s}}_{i,2} + L_{s_{i,3}}\hat{\boldsymbol{s}}_{i,3}$ is the net torque acting on the solar panel about its center of mass. The second differential equation is used to get the equations of motion of θ_i. The first and third equation could used to back-solve for the structural hinge torques embedded in $L_{s_{i,1}}$ and $L_{s_{i,3}}$ if needed.

Let $\boldsymbol{F}_{S_{c,i}}$ be the net force acting on the solar panel. Using the superparticle theorem[24] yields

$$\boldsymbol{F}_{S_{c,i}} = m_{\text{sp}_i}\ddot{\boldsymbol{r}}_{S_{c,i}/N} \tag{47}$$

The torque about the solar panel center of mass can be related to the torque about the hinge point H_i using

$$\boldsymbol{L}_{H_i} = \boldsymbol{L}_{S_{c,i}} + \boldsymbol{r}_{S_{c,i}/H_i} \times \boldsymbol{F}_{S_{c,i}} \tag{48}$$

Solving for the torque about $S_{c,i}$ yields

$$\boldsymbol{L}_{S_{c,i}} = \boldsymbol{L}_{H_i} - \boldsymbol{r}_{S_{c,i}/H_i} \times m_{\text{sp}_i}\ddot{\boldsymbol{r}}_{S_{c,i}/N} \tag{49}$$

Taking the vector dot product with $\hat{\boldsymbol{s}}_{i,2}$ and using $\boldsymbol{r}_{S_{c,i}/H_i} = -d_i\hat{\boldsymbol{s}}_{i,1}$ results in

$$L_{s_{i,2}} = \hat{\boldsymbol{s}}_{i,2} \cdot \boldsymbol{L}_{S_{c,i}} = \underbrace{\hat{\boldsymbol{s}}_{i,2} \cdot \boldsymbol{L}_{H_i}}_{L_{i,2}} - \hat{\boldsymbol{s}}_{i,2} \cdot \left(\boldsymbol{r}_{S_{c,i}/H_i} \times m_{\text{sp}_i}\ddot{\boldsymbol{r}}_{S_{c,i}/N}\right) \tag{50}$$

$$= -k_i\theta - c_i\dot{\theta}_i + \hat{\boldsymbol{s}}_{i,2} \cdot \boldsymbol{\tau}_{\text{ext},H_i} + m_{\text{sp}_i}d_i\hat{\boldsymbol{s}}_{i,2} \cdot \left(\hat{\boldsymbol{s}}_{i,1} \times \ddot{\boldsymbol{r}}_{S_{c,i}/N}\right) \tag{51}$$

Taking two inertial time derivatives of $\boldsymbol{r}_{S_{c,i}/N} = \boldsymbol{r}_{H_i/N} - d\hat{\boldsymbol{s}}_{i,1}$ yields

$$\ddot{\boldsymbol{r}}_{S_{c,i}/N} = \ddot{\boldsymbol{r}}_{H_i/N} - \dot{\boldsymbol{\omega}}_{\mathcal{S}_i/\mathcal{N}} \times (d\hat{\boldsymbol{s}}_{i,1}) - \boldsymbol{\omega}_{\mathcal{S}_i/\mathcal{N}} \times (\boldsymbol{\omega}_{\mathcal{S}_i/\mathcal{N}} \times (d\hat{\boldsymbol{s}}_{i,1})) \tag{52}$$

Substituting this inertial acceleration into the above $L_{s_{i,2}}$ expression provides

$$\begin{aligned} L_{s_{i,2}} = -k_i\theta - c_i\dot{\theta}_i + \hat{\boldsymbol{s}}_{i,2} \cdot \boldsymbol{\tau}_{\text{ext},H_i} + m_{\text{sp}_i}d_i\hat{\boldsymbol{s}}_{i,2} \cdot (\hat{\boldsymbol{s}}_{i,1} \times \ddot{\boldsymbol{r}}_{H_i/N}) + m_{\text{sp}_i}d_i^2\hat{\boldsymbol{s}}_{i,2} \cdot (\hat{\boldsymbol{s}}_{i,1} \times (\hat{\boldsymbol{s}}_{i,1} \times \dot{\boldsymbol{\omega}}_{\mathcal{S}_i/\mathcal{N}})) \\ - m_{\text{sp}_i}d_i^2\hat{\boldsymbol{s}}_{i,2} \cdot (\hat{\boldsymbol{s}}_{i,1} \times (\boldsymbol{\omega}_{\mathcal{S}_i/\mathcal{N}} \times (\boldsymbol{\omega}_{\mathcal{S}_i/\mathcal{N}} \times \hat{\boldsymbol{s}}_{i,1}))) \end{aligned} \tag{53}$$

Using the double vector cross product identity, as well as $\boldsymbol{a} \cdot (\boldsymbol{b} \times \boldsymbol{c}) = (\boldsymbol{a} \times \boldsymbol{b}) \cdot \boldsymbol{c}$, the $L_{s_{i,2}}$ torque component is simplified to

$$L_{s_{i,2}} = -k_i\theta - c_i\dot{\theta}_i + \hat{\boldsymbol{s}}_{i,2} \cdot \boldsymbol{\tau}_{\text{ext},H_i} - m_{\text{sp}_i}d_i\hat{\boldsymbol{s}}_{i,3} \cdot \ddot{\boldsymbol{r}}_{H_i/N} - m_{\text{sp}_i}d_i^2\hat{\boldsymbol{s}}_{i,2} \cdot \dot{\boldsymbol{\omega}}_{\mathcal{B}/\mathcal{N}} - m_{\text{sp}_i}d_i^2\ddot{\theta}_i + m_{\text{sp}_i}d_i^2\omega_{s_{i,3}}\omega_{s_{i,1}} \tag{54}$$

Substituting this torque into the earlier differential equation

$$I_{s_{i,2}}(\dot{\omega}_{s_{i,2}} + \ddot{\theta}_i) = -(I_{s_{i,1}} - I_{s_{i,3}})\omega_{s_{i,3}}\omega_{s_{i,1}} + L_{s_{i,2}} \tag{55}$$

leads to the desired scalar hinged solar panel equation of motion

$$\begin{aligned} \left(I_{s_{i,2}} + m_{\text{sp}_i}d_i^2\right)\hat{\boldsymbol{s}}_{i,2}^T\dot{\boldsymbol{\omega}}_{\mathcal{B}/\mathcal{N}} + \left(I_{s_{i,2}} + m_{\text{sp}_i}d_i^2\right)\ddot{\theta}_i + m_{\text{sp}_i}d_i\hat{\boldsymbol{s}}_{i,3}^T\ddot{\boldsymbol{r}}_{H_i/N} + k_i\theta + c_i\dot{\theta}_i - \hat{\boldsymbol{s}}_{i,2} \cdot \boldsymbol{\tau}_{\text{ext},H_i} \\ + \left(I_{s_{i,1}} - I_{s_{i,3}} - m_{\text{sp}_i}d_i^2\right)\omega_{s_{i,3}}\omega_{s_{i,1}} = 0 \end{aligned} \tag{56}$$

The term $\ddot{\boldsymbol{r}}_{H_i/N}$ needs to be expanded to be in terms of the desired translational motion $\ddot{\boldsymbol{r}}_{B/N}$. Knowing that the hinge location is a fixed point on the body, Eq. (56) is changed to the following form

$$\left(I_{s_{i,2}} + m_{\text{sp}_i} d_i^2\right) \hat{\boldsymbol{s}}_{i,2}^T \dot{\boldsymbol{\omega}}_{\mathcal{B}/\mathcal{N}} + m_{\text{sp}_i} d_i \hat{\boldsymbol{s}}_{i,3}^T (\ddot{\boldsymbol{r}}_{B/N} + \dot{\boldsymbol{\omega}}_{\mathcal{B}/\mathcal{N}} \times \boldsymbol{r}_{H_i/N} + \boldsymbol{\omega}_{\mathcal{B}/\mathcal{N}} \times (\boldsymbol{\omega}_{\mathcal{B}/\mathcal{N}} \times \boldsymbol{r}_{H_i/N}))$$
$$+ \left(I_{s_{i,2}} + m_{\text{sp}_i} d_i^2\right) \ddot{\theta}_i + k_i \theta_i + c_i \dot{\theta}_i - \hat{\boldsymbol{s}}_{i,2} \cdot \boldsymbol{\tau}_{\text{ext},H_i} + \left(I_{s_{i,1}} - I_{s_{i,3}} - m_{\text{sp}_i} d_i^2\right) \omega_{s_{i,3}} \omega_{s_{i,1}} = 0 \quad (57)$$

Following the same form introduced in the previous sections, the second order state variables are isolated to the left-hand side of the equation and the cross products are replaced with the skew symmetric matrices:

$$m_{\text{sp}_i} d_i \hat{\boldsymbol{s}}_{i,3}^T \ddot{\boldsymbol{r}}_{B/N} + \left[\left(I_{s_{i,2}} + m_{\text{sp}_i} d_i^2\right) \hat{\boldsymbol{s}}_{i,2}^T - m_{\text{sp}_i} d_i \hat{\boldsymbol{s}}_{i,3}^T [\tilde{\boldsymbol{r}}_{H_i/B}]\right] \dot{\boldsymbol{\omega}}_{\mathcal{B}/\mathcal{N}} + \left(I_{s_{i,2}} + m_{\text{sp}_i} d_i^2\right) \ddot{\theta}_i$$
$$= -k_i \theta_i - c_i \dot{\theta}_i + \hat{\boldsymbol{s}}_{i,2} \cdot \boldsymbol{\tau}_{\text{ext},H_i} + \left(I_{s_{i,3}} - I_{s_{i,1}} + m_{\text{sp}_i} d_i^2\right) \omega_{s_{i,3}} \omega_{s_{i,1}} - m_{\text{sp}_i} d_i \hat{\boldsymbol{s}}_{i,3}^T [\tilde{\boldsymbol{\omega}}_{\mathcal{B}/\mathcal{N}}][\tilde{\boldsymbol{\omega}}_{\mathcal{B}/\mathcal{N}}] \boldsymbol{r}_{H_i/B} \quad (58)$$

Eq. (58) is the third EOM required to describe the motion of the spacecraft and will be utilized later in the paper. The next section explains the formulation of the fuel slosh motion.

III.D Fuel Slosh Motion

The fuel slosh motion is being approximated by a lumped mechanical multi-mode model.[14,15,23] Figure 2(a) shows that a single fuel slosh particle is free to move along its corresponding $\hat{\boldsymbol{p}}_j$ direction and this formulation is generalized to include N_P number of fuel slosh particles. The derivation begins with Newton's law for each fuel slosh particle:

$$m_j \ddot{\boldsymbol{r}}_{P_{c,j}/N} = \boldsymbol{F}_G + \boldsymbol{F}_C - k_j \rho_j \hat{\boldsymbol{p}}_j - c_j \dot{\rho}_j \hat{\boldsymbol{p}}_j \quad (59)$$

Where $\boldsymbol{F}_G$ is the force of gravity and $\boldsymbol{F}_C$ is the constraint force that maintains the fuel slosh mass to travel along the direction $\hat{\boldsymbol{p}}_j$. The forces due to the spring and damper are explicitly included in Eq. (59) and result in a restoring force and damping force. $\ddot{\boldsymbol{r}}_{P_{c,j}/N}$ is defined in the following equation.

$$\ddot{\boldsymbol{r}}_{P_{c,j}/N} = \ddot{\boldsymbol{r}}_{B/N} + \ddot{\boldsymbol{r}}_{P_{c,j}/B} \quad (60)$$

The inertial acceleration vector $\ddot{\boldsymbol{r}}_{P_{c,j}/B}$ is defined in Eq. (24). Plugging this definition into Eq. (59) results in

$$m_j \left[\ddot{\boldsymbol{r}}_{B/N} + \ddot{\rho}_j \hat{\boldsymbol{p}}_j + 2\boldsymbol{\omega}_{\mathcal{B}/\mathcal{N}} \times \boldsymbol{r}'_{P_{c,j}/B} + \dot{\boldsymbol{\omega}}_{\mathcal{B}/\mathcal{N}} \times \boldsymbol{r}_{P_{c,j}/B} + \boldsymbol{\omega}_{\mathcal{B}/\mathcal{N}} \times (\boldsymbol{\omega}_{\mathcal{B}/\mathcal{N}} \times \boldsymbol{r}_{P_{c,j}/B})\right]$$
$$= \boldsymbol{F}_G + \boldsymbol{F}_C - k_j \rho_j \hat{\boldsymbol{p}}_j - c_j \dot{\rho}_j \hat{\boldsymbol{p}}_j \quad (61)$$

Equation (61) is the dynamical equation for a fuel slosh particle, however, the constraint force, $\boldsymbol{F}_C$, is undefined. Since the fuel slosh particle is free to move in the $\hat{\boldsymbol{p}}_j$ direction, the component of $\boldsymbol{F}_C$ along the $\hat{\boldsymbol{p}}_j$ direction is zero. Leveraging this insight, Eq. (61) is projected into the $\hat{\boldsymbol{p}}_j$ direction by multiplying both sides of the equation by $\hat{\boldsymbol{p}}_j{}^T$.

$$m_j \left(\hat{\boldsymbol{p}}_j{}^T \ddot{\boldsymbol{r}}_{B/N} + \ddot{\rho}_j + 2\hat{\boldsymbol{p}}_j{}^T \boldsymbol{\omega}_{\mathcal{B}/\mathcal{N}} \times \boldsymbol{r}'_{P_{c,j}/B} + \hat{\boldsymbol{p}}_j{}^T \dot{\boldsymbol{\omega}}_{\mathcal{B}/\mathcal{N}} \times \boldsymbol{r}_{P_{c,j}/B} + \hat{\boldsymbol{p}}_j{}^T \boldsymbol{\omega}_{\mathcal{B}/\mathcal{N}} \times (\boldsymbol{\omega}_{\mathcal{B}/\mathcal{N}} \times \boldsymbol{r}_{P_{c,j}/B})\right)$$
$$= \hat{\boldsymbol{p}}_j{}^T \boldsymbol{F}_G - k_j \rho_j - c_j \dot{\rho}_j \quad (62)$$

Moving the second order terms to the left hand side and introducing the tilde matrix notation yields the final equation needed to describe the motion of the spacecraft.

$$m_j \hat{\boldsymbol{p}}_j{}^T \ddot{\boldsymbol{r}}_{B/N} - m_j \hat{\boldsymbol{p}}_j{}^T [\tilde{\boldsymbol{r}}_{P_{c,j}/B}] \dot{\boldsymbol{\omega}}_{\mathcal{B}/\mathcal{N}} + m_j \ddot{\rho}_j$$
$$= \hat{\boldsymbol{p}}_j{}^T \boldsymbol{F}_G - k_j \rho_j - c_j \dot{\rho}_j - 2m_j \hat{\boldsymbol{p}}_j{}^T [\tilde{\boldsymbol{\omega}}_{\mathcal{B}/\mathcal{N}}] \boldsymbol{r}'_{P_{c,j}/B} - m_j \hat{\boldsymbol{p}}_j{}^T [\tilde{\boldsymbol{\omega}}_{\mathcal{B}/\mathcal{N}}][\tilde{\boldsymbol{\omega}}_{\mathcal{B}/\mathcal{N}}] \boldsymbol{r}_{P_{c,j}/B} \quad (63)$$

IV Back-substitution Method

The equations presented in the previous sections result in $N_S + N_P + 6$ coupled differential equations. Therefore, if the EOMs were placed into state space form, a system mass matrix of size $N_S + N_P + 6$ would need to be inverted to numerically integrate the EOMs. This can result in a computationally expensive simulation. The computation effort to numerically invert an $N \times N$ matrix scales with N^3. In the following section, the EOMs are manipulated using a back-substitution bethod to increase the computational efficiency.

To give a visual representation of the back-substitution method, Figure 3 is presented. This manipulation involves inverting an $N_S \times N_S$ matrix for the solar panel motion, inverting an $N_P \times N_P$ for the fuel slosh motion, inverting the rotational motion equation (3×3), and then back solving for the solar panel, fuel slosh and translational motions. The derivation of the back-substitution method can be seen in the following sections.

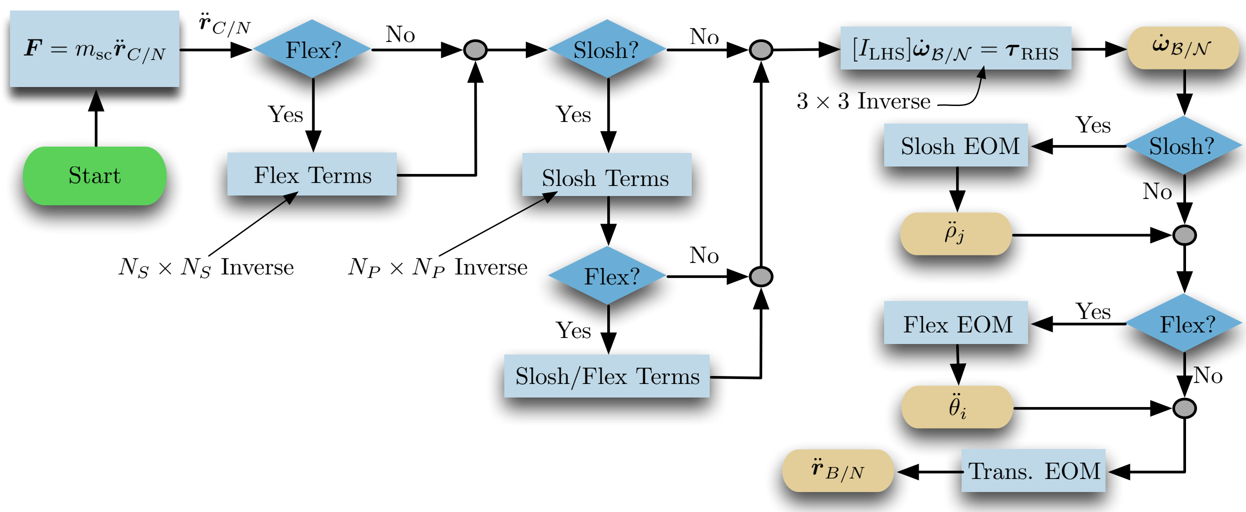

Figure 3: Back-substitution simulation implementation logic tree

IV.A Solar Panel and Fuel Slosh Motion

In Eq. (58), the solar panel motion is coupled with the translational motion and the rotational motion. The translational motion needs to be decoupled from the solar panel motion. To perform this task, Eq. (17) is substituted into Eq. (58).

$$\begin{aligned}
&m_{\text{sp}_i} d_i \hat{\boldsymbol{s}}_{i,3}^T \Big([\tilde{\boldsymbol{c}}]\dot{\boldsymbol{\omega}}_{\mathcal{B}/\mathcal{N}} - \frac{1}{m_{\text{sc}}} \sum_{i=1}^{N_S} m_{\text{sp}_i} d_i \hat{\boldsymbol{s}}_{i,3} \ddot{\theta}_i - \frac{1}{m_{\text{sc}}} \sum_{j=1}^{N_P} m_j \hat{\boldsymbol{p}}_j \ddot{\rho}_j + \ddot{\boldsymbol{r}}_{C/N} - 2[\tilde{\boldsymbol{\omega}}_{\mathcal{B}/\mathcal{N}}]\boldsymbol{c}' \\
&- [\tilde{\boldsymbol{\omega}}_{\mathcal{B}/\mathcal{N}}][\tilde{\boldsymbol{\omega}}_{\mathcal{B}/\mathcal{N}}]\boldsymbol{c} - \frac{1}{m_{\text{sc}}} \sum_{i=1}^{N_S} m_{\text{sp}_i} d_i \dot{\theta}_i^2 \hat{\boldsymbol{s}}_{i,1} \Big) + \Big[\left(I_{s_{i,2}} + m_{\text{sp}_i} d_i^2\right) \hat{\boldsymbol{s}}_{i,2}^T - m_{\text{sp}_i} d_i \hat{\boldsymbol{s}}_{i,3}^T [\tilde{\boldsymbol{r}}_{H_i/B}] \Big] \dot{\boldsymbol{\omega}}_{\mathcal{B}/\mathcal{N}} + \left(I_{s_{i,2}} + m_{\text{sp}_i} d_i^2\right) \ddot{\theta}_i \\
&= -k_i \theta_i - c_i \dot{\theta}_i + \left(I_{s_{i,3}} - I_{s_{i,1}} + m_{\text{sp}_i} d_i^2\right) \omega_{s_{i,3}} \omega_{s_{i,1}} - m_{\text{sp}_i} d_i \hat{\boldsymbol{s}}_{i,3}^T [\tilde{\boldsymbol{\omega}}_{\mathcal{B}/\mathcal{N}}][\tilde{\boldsymbol{\omega}}_{\mathcal{B}/\mathcal{N}}] \boldsymbol{r}_{H_i/B}
\end{aligned} \tag{64}$$

Isolating the second order solar panel variables and moving everything else to the right hand side results in

$$\begin{aligned}
&\Big(I_{s_{i,2}} + m_{\text{sp}_i} d_i^2 - \frac{m_{\text{sp}_i}^2}{m_{\text{sc}}} d_i^2\Big) \ddot{\theta}_i - \frac{m_{\text{sp}_i} d_i \hat{\boldsymbol{s}}_{i,3}^T}{m_{\text{sc}}} \sum_{k=1;k\neq i}^{N_S} m_{\text{sp}_k} d_k \hat{\boldsymbol{s}}_{k,3} \ddot{\theta}_k = -m_{\text{sp}_i} d_i \hat{\boldsymbol{s}}_{i,3}^T \Big([\tilde{\boldsymbol{c}}]\dot{\boldsymbol{\omega}}_{\mathcal{B}/\mathcal{N}} - \frac{1}{m_{\text{sc}}} \sum_{j=1}^{N_P} m_j \hat{\boldsymbol{p}}_j \ddot{\rho}_j + \ddot{\boldsymbol{r}}_{C/N} \\
&- 2[\tilde{\boldsymbol{\omega}}_{\mathcal{B}/\mathcal{N}}]\boldsymbol{c}' - [\tilde{\boldsymbol{\omega}}_{\mathcal{B}/\mathcal{N}}][\tilde{\boldsymbol{\omega}}_{\mathcal{B}/\mathcal{N}}]\boldsymbol{c} - \frac{1}{m_{\text{sc}}} \sum_{k=1;k\neq i}^{N_S} m_{\text{sp}_k} d_k \dot{\theta}_k^2 \hat{\boldsymbol{s}}_{k,1} \Big) - \Big[\left(I_{s_{i,2}} + m_{\text{sp}_i} d_i^2\right) \hat{\boldsymbol{s}}_{i,2}^T - m_{\text{sp}_i} d_i \hat{\boldsymbol{s}}_{i,3}^T [\tilde{\boldsymbol{r}}_{H_i/B}] \Big] \dot{\boldsymbol{\omega}}_{\mathcal{B}/\mathcal{N}} \\
&- k_i \theta_i - c_i \dot{\theta}_i + \left(I_{s_{i,3}} - I_{s_{i,1}} + m_{\text{sp}_i} d_i^2\right) \omega_{s_{i,3}} \omega_{s_{i,1}} - m_{\text{sp}_i} d_i \hat{\boldsymbol{s}}_{i,3}^T [\tilde{\boldsymbol{\omega}}_{\mathcal{B}/\mathcal{N}}][\tilde{\boldsymbol{\omega}}_{\mathcal{B}/\mathcal{N}}] \boldsymbol{r}_{H_i/B}
\end{aligned} \tag{65}$$

Combining second order terms on the right hand side yields

$$\begin{aligned}
&\Big(I_{s_{i,2}} + m_{\text{sp}_i} d_i^2 - \frac{m_{\text{sp}_i}^2}{m_{\text{sc}}} d_i^2\Big) \ddot{\theta}_i - \frac{m_{\text{sp}_i} d_i \hat{\boldsymbol{s}}_{i,3}^T}{m_{\text{sc}}} \sum_{k=1;k\neq i}^{N_S} m_{\text{sp}_k} d_k \hat{\boldsymbol{s}}_{k,3} \ddot{\theta}_k \\
&= -\Big[\left(I_{s_{i,2}} + m_{\text{sp}_i} d_i^2\right) \hat{\boldsymbol{s}}_{i,2}^T - m_{\text{sp}_i} d_i \hat{\boldsymbol{s}}_{i,3}^T \Big([\tilde{\boldsymbol{r}}_{H_i/B}] - [\tilde{\boldsymbol{c}}] \Big) \Big] \dot{\boldsymbol{\omega}}_{\mathcal{B}/\mathcal{N}} + \frac{m_{\text{sp}_i} d_i \hat{\boldsymbol{s}}_{i,3}^T}{m_{\text{sc}}} \sum_{j=1}^{N_P} m_j \hat{\boldsymbol{p}}_j \ddot{\rho}_j \\
&- m_{\text{sp}_i} d_i \hat{\boldsymbol{s}}_{i,3}^T \Big[\ddot{\boldsymbol{r}}_{C/N} - 2[\tilde{\boldsymbol{\omega}}_{\mathcal{B}/\mathcal{N}}]\boldsymbol{c}' + [\tilde{\boldsymbol{\omega}}_{\mathcal{B}/\mathcal{N}}][\tilde{\boldsymbol{\omega}}_{\mathcal{B}/\mathcal{N}}] \Big(\boldsymbol{r}_{H_i/B} - \boldsymbol{c} \Big) - \frac{1}{m_{\text{sc}}} \sum_{k=1;k\neq i}^{N_S} m_{\text{sp}_k} d_k \dot{\theta}_k^2 \hat{\boldsymbol{s}}_{k,1} \Big] \\
&- k_i \theta_i - c_i \dot{\theta}_i + \left(I_{s_{i,3}} - I_{s_{i,1}} + m_{\text{sp}_i} d_i^2\right) \omega_{s_{i,3}} \omega_{s_{i,1}}
\end{aligned} \tag{66}$$

Eq. (66) is written in matrix form to utilize some linear algebra techniques.

$$[A]\begin{bmatrix}\ddot{\theta}_1\\ \cdot\\ \cdot\\ \ddot{\theta}_{N_S}\end{bmatrix} = [F]\dot{\boldsymbol{\omega}}_{\mathcal{B}/\mathcal{N}} + [G]\begin{bmatrix}\ddot{\rho}_1\\ \cdot\\ \cdot\\ \ddot{\rho}_{N_P}\end{bmatrix} + \boldsymbol{v} \tag{67}$$

Where $[A]$ is an $N_S \times N_S$ matrix with the following definitions

$$a_{i,i} = I_{sp_{i,2}} + \Big(m_{\text{sp}_i} - \frac{m_{\text{sp}_i}^2}{m_{\text{sc}}}\Big)d_i^2 \tag{68a}$$

$$a_{i,k} = -\frac{m_{\text{sp}_i}}{m_{\text{sc}}} d_i \hat{\boldsymbol{s}}_{i,3}^T\big(m_{\text{sp}_k} d_k \hat{\boldsymbol{s}}_{k,3}\big) \tag{68b}$$

$[F]$ is an $N_S \times 3$ matrix with its row elements defined as

$$\boldsymbol{f}_i^T = -\Big[\big(I_{s_{i,2}} + m_{\text{sp}_i} d_i^2\big)\,\hat{\boldsymbol{s}}_{i,2}^T - m_{\text{sp}_i} d_i \hat{\boldsymbol{s}}_{i,3}^T\Big([\tilde{\boldsymbol{r}}_{H_i/B}] - [\tilde{\boldsymbol{c}}]\Big)\Big] \tag{69}$$

Here $[G]$ is an $N_S \times N_P$ matrix with the following definitions

$$g_{i,j} = \frac{m_{\text{sp}_i} d_i \hat{\boldsymbol{s}}_{i,3}^T}{m_{\text{sc}}} m_j \hat{\boldsymbol{p}}_j \tag{70}$$

The parameter $\boldsymbol{v}$ is an $N_S \times 1$ matrix with the following elements

$$v_i = -m_{\text{sp}_i} d_i \hat{\boldsymbol{s}}_{i,3}^T\Big[\ddot{\boldsymbol{r}}_{C/N} - 2[\tilde{\boldsymbol{\omega}}_{\mathcal{B}/\mathcal{N}}]\boldsymbol{c}' + [\tilde{\boldsymbol{\omega}}_{\mathcal{B}/\mathcal{N}}][\tilde{\boldsymbol{\omega}}_{\mathcal{B}/\mathcal{N}}]\Big(\boldsymbol{r}_{H_i/B} - \boldsymbol{c}\Big) - \frac{1}{m_{\text{sc}}}\sum_{k=1;k\neq i}^{N_S} m_{\text{sp}_k} d_k \dot{\theta}_k^2 \hat{\boldsymbol{s}}_{k,1}\Big]$$
$$- k_i\theta_i - c_i\dot{\theta}_i + \hat{\boldsymbol{s}}_{i,2}\cdot\boldsymbol{\tau}_{\text{ext},H_i} + \big(I_{s_{i,3}} - I_{s_{i,1}} + m_{\text{sp}_i} d_i^2\big)\,\omega_{s_{i,3}}\omega_{s_{i,1}} \tag{71}$$

Eq. (67) can now be solved by inverting matrix $[A]$. Note the definition $[E] = [A]^{-1}$.

$$\begin{bmatrix}\ddot{\theta}_1\\ \cdot\\ \cdot\\ \ddot{\theta}_{N_S}\end{bmatrix} = [E][F]\dot{\boldsymbol{\omega}}_{\mathcal{B}/\mathcal{N}} + [E][G]\begin{bmatrix}\ddot{\rho}_1\\ \cdot\\ \cdot\\ \ddot{\rho}_{N_P}\end{bmatrix} + [E]\boldsymbol{v} \tag{72}$$

Since the modified Euler's equation, Eq. (36), has $\ddot{\theta}_i$ terms, it is more convenient to use the expression for $\ddot{\theta}_i$ as

$$\ddot{\theta}_i = \boldsymbol{e}_i^T[F]\dot{\boldsymbol{\omega}}_{\mathcal{B}/\mathcal{N}} + \boldsymbol{e}_i^T[G]\begin{bmatrix}\ddot{\rho}_1\\ \cdot\\ \cdot\\ \ddot{\rho}_{N_P}\end{bmatrix} + \boldsymbol{e}_i^T\boldsymbol{v} \tag{73}$$

Where the subcomponents of $[E]$ are defined as

$$[E] = \begin{bmatrix}\boldsymbol{e}_1^T\\ \cdot\\ \cdot\\ \boldsymbol{e}_{N_S}^T\end{bmatrix} \tag{74}$$

The next step required is to decouple the translational and solar panel motions from the slosh EOM. Substituting the translational motion into the slosh equation, Eq. (63), results in

$$m_j\hat{\boldsymbol{p}}_j{}^T\Big([\tilde{\boldsymbol{c}}]\dot{\boldsymbol{\omega}}_{\mathcal{B}/\mathcal{N}} - \frac{1}{m_{\text{sc}}}\sum_{i=1}^{N_S} m_{\text{sp}_i} d_i \hat{\boldsymbol{s}}_{i,3}\ddot{\theta}_i - \frac{1}{m_{\text{sc}}}\sum_{j=1}^{N_P} m_j \hat{\boldsymbol{p}}_j \ddot{\rho}_j + \ddot{\boldsymbol{r}}_{C/N} - 2[\tilde{\boldsymbol{\omega}}_{\mathcal{B}/\mathcal{N}}]\boldsymbol{c}'$$
$$- [\tilde{\boldsymbol{\omega}}_{\mathcal{B}/\mathcal{N}}][\tilde{\boldsymbol{\omega}}_{\mathcal{B}/\mathcal{N}}]\boldsymbol{c} - \frac{1}{m_{\text{sc}}}\sum_{i=1}^{N_S} m_{\text{sp}_i} d_i \dot{\theta}_i^2 \hat{\boldsymbol{s}}_{i,1}\Big) - m_j\hat{\boldsymbol{p}}_j{}^T[\tilde{\boldsymbol{r}}_{P_{c,j}/B}]\dot{\boldsymbol{\omega}}_{\mathcal{B}/\mathcal{N}} + m_j\ddot{\rho}_j$$
$$= \hat{\boldsymbol{p}}_j{}^T\boldsymbol{F}_G - k_j\rho_j - c_j\dot{\rho}_j - 2m_j\hat{\boldsymbol{p}}_j{}^T[\tilde{\boldsymbol{\omega}}_{\mathcal{B}/\mathcal{N}}]\boldsymbol{r}'_{P_{c,j}/B} - m_j\hat{\boldsymbol{p}}_j{}^T[\tilde{\boldsymbol{\omega}}_{\mathcal{B}/\mathcal{N}}][\tilde{\boldsymbol{\omega}}_{\mathcal{B}/\mathcal{N}}]\boldsymbol{r}_{P_{c,j}/B} \tag{75}$$

Replacing the second order solar panel variables with Eq. (73) yields

$$m_j\hat{\boldsymbol{p}}_j^T\Big[[\tilde{\boldsymbol{c}}]\dot{\boldsymbol{\omega}}_{\mathcal{B}/\mathcal{N}}-\frac{1}{m_{\text{sc}}}\sum_{i=1}^{N_S}m_{\text{sp}_i}d_i\hat{\boldsymbol{s}}_{i,3}\Big(\boldsymbol{e}_i^T[F]\dot{\boldsymbol{\omega}}_{\mathcal{B}/\mathcal{N}}+\sum_{k=1}^{N_S}e_{i,k}\sum_{l=1}^{N_P}g_{k,l}\ddot{\rho}_l+\boldsymbol{e}_i^T\boldsymbol{v}\Big)-\frac{1}{m_{\text{sc}}}\sum_{l=1}^{N_P}m_l\hat{\boldsymbol{p}}_l\ddot{\rho}_l+\ddot{\boldsymbol{r}}_{C/N}-2[\tilde{\boldsymbol{\omega}}_{\mathcal{B}/\mathcal{N}}]\boldsymbol{c}'$$
$$-[\tilde{\boldsymbol{\omega}}_{\mathcal{B}/\mathcal{N}}][\tilde{\boldsymbol{\omega}}_{\mathcal{B}/\mathcal{N}}]\boldsymbol{c}-\frac{1}{m_{\text{sc}}}\sum_{i=1}^{N_S}m_{\text{sp}_i}d_i\dot{\theta}_i^2\hat{\boldsymbol{s}}_{i,1}\Big]-m_j\hat{\boldsymbol{p}}_j^T[\tilde{\boldsymbol{r}}_{P_{c,j}/B}]\dot{\boldsymbol{\omega}}_{\mathcal{B}/\mathcal{N}}+m_j\ddot{\rho}_j$$
$$=\hat{\boldsymbol{p}}_j^T\boldsymbol{F}_G-k_j\rho_j-c_j\dot{\rho}_j-2m_j\hat{\boldsymbol{p}}_j^T[\tilde{\boldsymbol{\omega}}_{\mathcal{B}/\mathcal{N}}]\boldsymbol{r}'_{P_{c,j}/B}-m_j\hat{\boldsymbol{p}}_j^T[\tilde{\boldsymbol{\omega}}_{\mathcal{B}/\mathcal{N}}][\tilde{\boldsymbol{\omega}}_{\mathcal{B}/\mathcal{N}}]\boldsymbol{r}_{P_{c,j}/B}\tag{76}$$

Isolating fuel slosh second order terms to the left hand side and combining $\dot{\boldsymbol{\omega}}_{\mathcal{B}/\mathcal{N}}$ terms on the right hand side of the equation yields

$$\Big[m_j-\frac{m_j^2}{m_{\text{sc}}}-\frac{m_j\hat{\boldsymbol{p}}_j^T}{m_{\text{sc}}}\sum_{i=1}^{N_S}m_{\text{sp}_i}d_i\hat{\boldsymbol{s}}_{i,3}\sum_{k=1}^{N_S}e_{i,k}g_{k,j}\Big]\ddot{\rho}_j-\frac{m_j\hat{\boldsymbol{p}}_j^T}{m_{\text{sc}}}\sum_{l=1;l\neq j}^{N_P}\Big[\Big(\sum_{i=1}^{N_S}m_{\text{sp}_i}d_i\hat{\boldsymbol{s}}_{i,3}\sum_{k=1}^{N_S}e_{i,k}g_{k,l}+m_l\hat{\boldsymbol{p}}_l\Big)\ddot{\rho}_l\Big]$$
$$=-m_j\hat{\boldsymbol{p}}_j^T\Big([\tilde{\boldsymbol{c}}]-[\tilde{\boldsymbol{r}}_{P_{c,j}/B}]-\frac{1}{m_{\text{sc}}}\sum_{i=1}^{N_S}m_{\text{sp}_i}d_i\hat{\boldsymbol{s}}_{i,3}\boldsymbol{e}_i^T[F]\Big)\dot{\boldsymbol{\omega}}_{\mathcal{B}/\mathcal{N}}$$
$$-m_j\hat{\boldsymbol{p}}_j^T\Big(-\frac{1}{m_{\text{sc}}}\sum_{i=1}^{N_S}m_{\text{sp}_i}d_i\Big[\hat{\boldsymbol{s}}_{i,3}\boldsymbol{e}_i^T\boldsymbol{v}+\dot{\theta}_i^2\hat{\boldsymbol{s}}_{i,1}\Big]+\ddot{\boldsymbol{r}}_{C/N}-\frac{\boldsymbol{F}_G}{m_j}+2[\tilde{\boldsymbol{\omega}}_{\mathcal{B}/\mathcal{N}}]\Big[\boldsymbol{r}'_{P_{c,j}/B}-\boldsymbol{c}'\Big]$$
$$+[\tilde{\boldsymbol{\omega}}_{\mathcal{B}/\mathcal{N}}][\tilde{\boldsymbol{\omega}}_{\mathcal{B}/\mathcal{N}}]\Big[\boldsymbol{r}_{P_{c,j}/B}-\boldsymbol{c}\Big]\Big)-k_j\rho_j-c_j\dot{\rho}_j\tag{77}$$

Eq. (77) is written in matrix form

$$[N]\begin{bmatrix}\ddot{\rho}_1\\ \cdot\\ \cdot\\ \ddot{\rho}_{N_P}\end{bmatrix}=[O]\dot{\boldsymbol{\omega}}_{\mathcal{B}/\mathcal{N}}+\boldsymbol{q}\tag{78}$$

Where $[N]$ is an $N_P\times N_P$ matrix with the following definitions

$$n_{j,j}=m_j-\frac{m_j^2}{m_{\text{sc}}}-\frac{m_j\hat{\boldsymbol{p}}_j^T}{m_{\text{sc}}}\sum_{i=1}^{N_S}m_{\text{sp}_i}d_i\hat{\boldsymbol{s}}_{i,3}\sum_{k=1}^{N_S}e_{i,k}g_{k,j}\tag{79a}$$

$$n_{j,l}=-\frac{m_j\hat{\boldsymbol{p}}_j^T}{m_{\text{sc}}}\Big(\sum_{i=1}^{N_S}m_{\text{sp}_i}d_i\hat{\boldsymbol{s}}_{i,3}\sum_{k=1}^{N_S}e_{i,k}g_{k,l}+m_l\hat{\boldsymbol{p}}_l\Big)\tag{79b}$$

$[O]$ is an $N_P\times 3$ matrix with its row elements defined as

$$\boldsymbol{o}_j^T=-m_j\hat{\boldsymbol{p}}_j^T\Big([\tilde{\boldsymbol{c}}]-[\tilde{\boldsymbol{r}}_{P_{c,j}/B}]-\frac{1}{m_{\text{sc}}}\sum_{i=1}^{N_S}m_{\text{sp}_i}d_i\hat{\boldsymbol{s}}_{i,3}\boldsymbol{e}_i^T[F]\Big)\tag{80}$$

$\boldsymbol{q}$ is an $N_P\times 1$ vector with the following elements

$$q_j=-m_j\hat{\boldsymbol{p}}_j^T\Big(-\frac{1}{m_{\text{sc}}}\sum_{i=1}^{N_S}m_{\text{sp}_i}d_i\Big[\hat{\boldsymbol{s}}_{i,3}\boldsymbol{e}_i^T\boldsymbol{v}+\dot{\theta}_i^2\hat{\boldsymbol{s}}_{i,1}\Big]+\ddot{\boldsymbol{r}}_{C/N}-\frac{\boldsymbol{F}_G}{m_j}+2[\tilde{\boldsymbol{\omega}}_{\mathcal{B}/\mathcal{N}}]\Big[\boldsymbol{r}'_{P_{c,j}/B}-\boldsymbol{c}'\Big]$$
$$+[\tilde{\boldsymbol{\omega}}_{\mathcal{B}/\mathcal{N}}][\tilde{\boldsymbol{\omega}}_{\mathcal{B}/\mathcal{N}}]\Big[\boldsymbol{r}_{P_{c,j}/B}-\boldsymbol{c}\Big]\Big)-k_j\rho_j-c_j\dot{\rho}_j\tag{81}$$

Inverting matrix $[N]$ ($[T]=[N]^{-1}$) solves the equation for second order slosh terms

$$\begin{bmatrix}\ddot{\rho}_1\\ \cdot\\ \cdot\\ \ddot{\rho}_{N_P}\end{bmatrix}=[T][O]\dot{\boldsymbol{\omega}}_{\mathcal{B}/\mathcal{N}}+[T]\boldsymbol{q}\tag{82}$$

It is also convenient to write the slosh equations in the following form

$$\ddot{\rho}_j = \boldsymbol{t}_j^T [O]\dot{\boldsymbol{\omega}}_{\mathcal{B}/\mathcal{N}} + \boldsymbol{t}_j^T \boldsymbol{q} \tag{83}$$

Where the subcomponents of $[T]$ are defined as

$$[T] = \begin{bmatrix} \boldsymbol{t}_1^T \\ \cdot \\ \cdot \\ \boldsymbol{t}_{N_P}^T \end{bmatrix} \tag{84}$$

IV.B Hub Rotational Motion

The rotational motion is coupled with the solar panel, fuel slosh and translational motions. Therefore, the translational, solar panel, and fuel slosh EOMs need to be substituted into the modified Euler's equation, Eq. (36). First, the translational motion is substituted into Eq. (36).

$$\begin{aligned} m_{\text{sc}}[\tilde{\boldsymbol{c}}]\Bigg([\tilde{\boldsymbol{c}}]\dot{\boldsymbol{\omega}}_{\mathcal{B}/\mathcal{N}} - \frac{1}{m_{\text{sc}}}\sum_{i=1}^{N_S} m_{\text{sp}_i} d_i \hat{\boldsymbol{s}}_{i,3}\ddot{\theta}_i - \frac{1}{m_{\text{sc}}}\sum_{j=1}^{N_P} m_j \hat{\boldsymbol{p}}_j \ddot{\rho}_j + \ddot{\boldsymbol{r}}_{C/N} - 2[\tilde{\boldsymbol{\omega}}_{\mathcal{B}/\mathcal{N}}]\boldsymbol{c}' \\ -[\tilde{\boldsymbol{\omega}}_{\mathcal{B}/\mathcal{N}}][\tilde{\boldsymbol{\omega}}_{\mathcal{B}/\mathcal{N}}]\boldsymbol{c} - \frac{1}{m_{\text{sc}}}\sum_{i=1}^{N_S} m_{\text{sp}_i} d_i \dot{\theta}_i^2 \hat{\boldsymbol{s}}_{i,1}\Bigg) + [I_{\text{sc},B}]\dot{\boldsymbol{\omega}}_{\mathcal{B}/\mathcal{N}} + \sum_{i=1}^{N_S}\Big\{I_{S_{c,i},2}\hat{\boldsymbol{s}}_{i,2} + m_{\text{sp}_i} d_i [\tilde{\boldsymbol{r}}_{S_{c,i}/B}]\hat{\boldsymbol{s}}_{i,3}\Big\}\ddot{\theta}_i + \sum_{j=1}^{N_P} m_j [\tilde{\boldsymbol{r}}_{P_{c,j}/B}]\hat{\boldsymbol{p}}_j \ddot{\rho}_j = \\ -[\tilde{\boldsymbol{\omega}}_{\mathcal{B}/\mathcal{N}}][I_{\text{sc},B}]\boldsymbol{\omega}_{\mathcal{B}/\mathcal{N}} - [I'_{\text{sc},B}]\boldsymbol{\omega}_{\mathcal{B}/\mathcal{N}} - \sum_{i=1}^{N_S}\Big\{\dot{\theta}_i [\tilde{\boldsymbol{\omega}}_{\mathcal{B}/\mathcal{N}}]\left(I_{S_{c,i},2}\hat{\boldsymbol{s}}_{i,2} + m_{\text{sp}_i} d_i [\tilde{\boldsymbol{r}}_{S_{c,i}/B}]\hat{\boldsymbol{s}}_{i,3}\right) \\ + m_{\text{sp}_i} d_i \dot{\theta}_i^2 [\tilde{\boldsymbol{r}}_{S_{c,i}/B}]\hat{\boldsymbol{s}}_{i,1}\Big\} - \sum_{j=1}^{N_P} m_j [\tilde{\boldsymbol{\omega}}_{\mathcal{B}/\mathcal{N}}][\tilde{\boldsymbol{r}}_{P_{c,j}/B}]\boldsymbol{r}'_{P_{c,j}/B} + \boldsymbol{L}_B \end{aligned} \tag{85}$$

Second order variables are combined

$$\begin{aligned} \Big([I_{\text{sc},B}] + m_{\text{sc}}[\tilde{\boldsymbol{c}}][\tilde{\boldsymbol{c}}]\Big)\dot{\boldsymbol{\omega}}_{\mathcal{B}/\mathcal{N}} + \sum_{i=1}^{N_S}\Big\{I_{S_{c,i},2}\hat{\boldsymbol{s}}_{i,2} + m_{\text{sp}_i} d_i \Big([\tilde{\boldsymbol{r}}_{S_{c,i}/B}] - [\tilde{\boldsymbol{c}}]\Big)\hat{\boldsymbol{s}}_{i,3}\Big\}\ddot{\theta}_i + \sum_{j=1}^{N_P} m_j \Big([\tilde{\boldsymbol{r}}_{P_{c,j}/B}] - [\tilde{\boldsymbol{c}}]\Big)\hat{\boldsymbol{p}}_j \ddot{\rho}_j \\ + m_{\text{sc}}[\tilde{\boldsymbol{c}}]\Bigg(\ddot{\boldsymbol{r}}_{C/N} - 2[\tilde{\boldsymbol{\omega}}_{\mathcal{B}/\mathcal{N}}]\boldsymbol{c}' - [\tilde{\boldsymbol{\omega}}_{\mathcal{B}/\mathcal{N}}][\tilde{\boldsymbol{\omega}}_{\mathcal{B}/\mathcal{N}}]\boldsymbol{c} - \frac{1}{m_{\text{sc}}}\sum_{i=1}^{N_S} m_{\text{sp}_i} d_i \dot{\theta}_i^2 \hat{\boldsymbol{s}}_{i,1}\Bigg) = \\ -[\tilde{\boldsymbol{\omega}}_{\mathcal{B}/\mathcal{N}}][I_{\text{sc},B}]\boldsymbol{\omega}_{\mathcal{B}/\mathcal{N}} - [I'_{\text{sc},B}]\boldsymbol{\omega}_{\mathcal{B}/\mathcal{N}} - \sum_{i=1}^{N_S}\Big\{\dot{\theta}_i [\tilde{\boldsymbol{\omega}}_{\mathcal{B}/\mathcal{N}}]\left(I_{S_{c,i},2}\hat{\boldsymbol{s}}_{i,2} + m_{\text{sp}_i} d_i [\tilde{\boldsymbol{r}}_{S_{c,i}/B}]\hat{\boldsymbol{s}}_{i,3}\right) \\ + m_{\text{sp}_i} d_i \dot{\theta}_i^2 [\tilde{\boldsymbol{r}}_{S_{c,i}/B}]\hat{\boldsymbol{s}}_{i,1}\Big\} - \sum_{j=1}^{N_P} m_j [\tilde{\boldsymbol{\omega}}_{\mathcal{B}/\mathcal{N}}][\tilde{\boldsymbol{r}}_{P_{c,j}/B}]\boldsymbol{r}'_{P_{c,j}/B} + \boldsymbol{L}_B \end{aligned} \tag{86}$$

Next Eqs. (73) and (83) are substituted into Eq. (86) and the $\dot{\boldsymbol{\omega}}_{\mathcal{B}/\mathcal{N}}$ terms are isolated to the left hand side of the equation

$$\Big\{[I_{\text{sc},B}] + m_{\text{sc}}[\tilde{\boldsymbol{c}}][\tilde{\boldsymbol{c}}] + \sum_{i=1}^{N_S}\Big[I_{S_{c,i},2}\hat{\boldsymbol{s}}_{i,2} + m_{\text{sp}_i}d_i\Big([\tilde{\boldsymbol{r}}_{S_{c,i}/B}] - [\tilde{\boldsymbol{c}}]\Big)\hat{\boldsymbol{s}}_{i,3}\Big]\Big(\boldsymbol{e}_i^T[F] + \boldsymbol{e}_i^T[G][T][O]\Big)$$
$$+ \sum_{j=1}^{N_P} m_j\Big([\tilde{\boldsymbol{r}}_{P_{c,j}/B}] - [\tilde{\boldsymbol{c}}]\Big)\hat{\boldsymbol{p}}_j\boldsymbol{t}_j^T[O]\Big\}\dot{\boldsymbol{\omega}}_{\mathcal{B}/\mathcal{N}} = -[\tilde{\boldsymbol{\omega}}_{\mathcal{B}/\mathcal{N}}][I_{\text{sc},B}]\boldsymbol{\omega}_{\mathcal{B}/\mathcal{N}} - [I'_{\text{sc},B}]\boldsymbol{\omega}_{\mathcal{B}/\mathcal{N}} + \boldsymbol{L}_B$$
$$-m_{\text{sc}}[\tilde{\boldsymbol{c}}]\Big(\ddot{\boldsymbol{r}}_{C/N} - 2[\tilde{\boldsymbol{\omega}}_{\mathcal{B}/\mathcal{N}}]\boldsymbol{c}' - [\tilde{\boldsymbol{\omega}}_{\mathcal{B}/\mathcal{N}}][\tilde{\boldsymbol{\omega}}_{\mathcal{B}/\mathcal{N}}]\boldsymbol{c}\Big) - \sum_{i=1}^{N_S}\Big\{\Big[I_{S_{c,i},2}\hat{\boldsymbol{s}}_{i,2} + m_{\text{sp}_i}d_i\Big([\tilde{\boldsymbol{r}}_{S_{c,i}/B}] - [\tilde{\boldsymbol{c}}]\Big)\hat{\boldsymbol{s}}_{i,3}\Big]\Big[\boldsymbol{e}_i^T[G][T]\boldsymbol{q} + \boldsymbol{e}_i^T\boldsymbol{v}\Big]$$
$$+ \dot{\theta}_i[\tilde{\boldsymbol{\omega}}_{\mathcal{B}/\mathcal{N}}]\left(I_{S_{c,i},2}\hat{\boldsymbol{s}}_{i,2} + m_{\text{sp}_i}d_i[\tilde{\boldsymbol{r}}_{S_{c,i}/B}]\hat{\boldsymbol{s}}_{i,3}\right) + m_{\text{sp}_i}d_i\dot{\theta}_i^2\Big([\tilde{\boldsymbol{r}}_{S_{c,i}/B}] - [\tilde{\boldsymbol{c}}]\Big)\hat{\boldsymbol{s}}_{i,1}\Big\}$$
$$- \sum_{j=1}^{N_P} m_j\Big\{[\tilde{\boldsymbol{\omega}}_{\mathcal{B}/\mathcal{N}}][\tilde{\boldsymbol{r}}_{P_{c,j}/B}]\boldsymbol{r}'_{P_{c,j}/B} + \Big([\tilde{\boldsymbol{r}}_{P_{c,j}/B}] - [\tilde{\boldsymbol{c}}]\Big)\hat{\boldsymbol{p}}_j\boldsymbol{t}_j^T\boldsymbol{q}\Big\} \quad (87)$$

Here $[R]$ is a $3 \times N_S$ matrix with its column elements defined as

$$\boldsymbol{R}_i = I_{s_i,2}\hat{\boldsymbol{s}}_{i,2} + m_{\text{sp}_i}d_i\left([\tilde{\boldsymbol{r}}_{S_i/B}] - [\tilde{\boldsymbol{c}}]\right)\hat{\boldsymbol{s}}_{i,3} \quad (88)$$

and $[X]$ is a $3 \times N_P$ matrix with its column elements defined as

$$\boldsymbol{x}_j = m_j\Big([\tilde{\boldsymbol{r}}_{P_{c,j}/B}] - [\tilde{\boldsymbol{c}}]\Big)\hat{\boldsymbol{p}}_j \quad (89)$$

The following definitions are defined to simplify the EOM to

$$[I_{\text{LHS}}] = [I_{\text{sc},B}] + m_{\text{sc}}[\tilde{\boldsymbol{c}}][\tilde{\boldsymbol{c}}] + \sum_{i=1}^{N_S}\boldsymbol{R}_i\Big(\boldsymbol{e}_i^T[F] + \boldsymbol{e}_i^T[G][T][O]\Big) + \sum_{j=1}^{N_P}\boldsymbol{x}_j\boldsymbol{t}_j^T[O] \quad (90)$$

$$\boldsymbol{\tau}_{\text{RHS}} = -[\tilde{\boldsymbol{\omega}}_{\mathcal{B}/\mathcal{N}}][I_{\text{sc},B}]\boldsymbol{\omega}_{\mathcal{B}/\mathcal{N}} - [I'_{\text{sc},B}]\boldsymbol{\omega}_{\mathcal{B}/\mathcal{N}} + \boldsymbol{L}_B$$
$$- m_{\text{sc}}[\tilde{\boldsymbol{c}}]\Big(\ddot{\boldsymbol{r}}_{C/N} - 2[\tilde{\boldsymbol{\omega}}_{\mathcal{B}/\mathcal{N}}]\boldsymbol{c}' - [\tilde{\boldsymbol{\omega}}_{\mathcal{B}/\mathcal{N}}][\tilde{\boldsymbol{\omega}}_{\mathcal{B}/\mathcal{N}}]\boldsymbol{c}\Big) - \sum_{i=1}^{N_S}\Big\{\boldsymbol{R}_i\Big[\boldsymbol{e}_i^T[G][T]\boldsymbol{q} + \boldsymbol{e}_i^T\boldsymbol{v}\Big]$$
$$+ \dot{\theta}_i[\tilde{\boldsymbol{\omega}}_{\mathcal{B}/\mathcal{N}}]\left(I_{S_{c,i},2}\hat{\boldsymbol{s}}_{i,2} + m_{\text{sp}_i}d_i[\tilde{\boldsymbol{r}}_{S_{c,i}/B}]\hat{\boldsymbol{s}}_{i,3}\right) + m_{\text{sp}_i}d_i\dot{\theta}_i^2\Big([\tilde{\boldsymbol{r}}_{S_{c,i}/B}] - [\tilde{\boldsymbol{c}}]\Big)\hat{\boldsymbol{s}}_{i,1}\Big\}$$
$$- \sum_{j=1}^{N_P}\Big\{m_j[\tilde{\boldsymbol{\omega}}_{\mathcal{B}/\mathcal{N}}][\tilde{\boldsymbol{r}}_{P_{c,j}/B}]\boldsymbol{r}'_{P_{c,j}/B} + \boldsymbol{x}_j\boldsymbol{t}_j^T\boldsymbol{q}\Big\} \quad (91)$$

$[I_{\text{LHS}}]$ is a 3×3 matrix and $\boldsymbol{\tau}_{\text{RHS}}$ is a 3×1 vector. This allows the final equation to be simplified to the following form

$$[I_{\text{LHS}}]\dot{\boldsymbol{\omega}}_{\mathcal{B}/\mathcal{N}} = \boldsymbol{\tau}_{\text{RHS}} \quad (92)$$

IV.C Remaining Back-substitution Steps

Now Eq. (92) can be solved for $\dot{\boldsymbol{\omega}}_{\mathcal{B}/\mathcal{N}}$. It is important to note that there are three remaining steps required to implement these equations into a simulation. $\dot{\boldsymbol{\omega}}_{\mathcal{B}/\mathcal{N}}$ is placed into the fuel slosh motion equation, Eq. (83), to solve for $\ddot{\rho}_j$. The solutions for $\dot{\boldsymbol{\omega}}_{\mathcal{B}/\mathcal{N}}$ and $\ddot{\rho}_j$ are placed into Eq. (73) to solve for $\ddot{\theta}_i$. And finally, the solution for $\ddot{\theta}_i$, $\ddot{\rho}_j$ and $\dot{\boldsymbol{\omega}}_{\mathcal{B}/\mathcal{N}}$ are placed into the translational motion equation, Eq. (17), to solve for $\ddot{\boldsymbol{r}}_{B/N}$. This concludes the necessary steps needed to implement flexible and fuel slosh dynamics into a computer simulation. The recommended coordinate frames for this simulation are to solve everything in the body frame, $\mathcal{B}$, and before integration, place the translational motion in the inertial frame, $\mathcal{N}$. However, this formulation is general, and any coordinate frames can be chosen as needed.

Table 1: Hub simulation parameters

Hub	m_{hub} $[kg]$	750
	$[I_{\text{hub},B_c}]$ $[kg\text{-}m^2]$	$\text{diag}([900 \quad 800 \quad 600])$
	${}^{\mathcal{B}}\boldsymbol{r}_{B_c/B}$	$[0.00133 \quad -0.267 \quad 0]^T$

Table 2: Solar panel simulation parameters

Solar Panels	$m_{\text{sp}_1}, m_{\text{sp}_2}$ $[kg]$	100
	$[I_{S_{c,1}}], [I_{S_{c,2}}]$ $[kg\text{-}m^2]$	$\text{diag}([100 \quad 50 \quad 50])$
	${}^{\mathcal{B}}\boldsymbol{r}_{H_1/N}$ $[m]$	$[0.5 \quad 1 \quad 0]^T$
	${}^{\mathcal{B}}\boldsymbol{r}_{H_2/N}$ $[m]$	$[-0.5 \quad 1 \quad 0]^T$
	$[H_1B]$	$\begin{bmatrix} -1 & 0 & 0 \\ 0 & 0 & 1 \\ 0 & 1 & 0 \end{bmatrix}$
	$[H_2B]$	$\begin{bmatrix} 1 & 0 & 0 \\ 0 & 0 & -1 \\ 0 & 1 & 0 \end{bmatrix}$
	d_1, d_2 $[m]$	1.5
	k_1, k_2 $[N]$	43426.26
	c_1, c_2 $[Ns]$	138.23

Table 3: Slosh simulation parameters

Slosh modes	m_1, m_2 $[kg]$	10, 20
	${}^{\mathcal{B}}\boldsymbol{r}_{P_{c,1}/B}$ $[m]$	$[0.1 \quad 0 \quad 0]^T$
	${}^{\mathcal{B}}\boldsymbol{r}_{P_{c,2}/B}$ $[m]$	$[-0.1 \quad 0 \quad 0]^T$
	${}^{\mathcal{B}}\hat{\boldsymbol{p}}_1, {}^{\mathcal{B}}\hat{\boldsymbol{p}}_2$	$[0 \quad 1 \quad 0]^T$
	k_1, k_2 $[N/m]$	3.95, 71.06
	c_1, c_2 $[Ns/m]$	2.51, 7.54

V Numerical Simulation

In order to validate the EOMs and to provide a simple example of the flexing and slosh behavior, a numerical simulation is setup. The spacecraft is composed by a hub, two solar panels, and two slosh masses. The parameters used for the simulation can be seen in Tables 1-3. Two different simulations are run: with and without damping. The table shows the damping parameters for the damped case. For the undamped case they are all zero.

For simplicity, the spacecraft is given initial conditions that will constrain its movement to planar motion. No external forces are acting on the body. The non-zero initial values are $\theta_{1_0} = 5°$, $\rho_{1_0} = 5$ cm, $\rho_{2_0} = -2.5$ cm. All other initial values are set to zero.

To describe the one-dimensional planar rotation, the angle between $\hat{\boldsymbol{b}}_3$ and $\hat{\boldsymbol{n}}_3$ is defined as ϕ. It should be noted

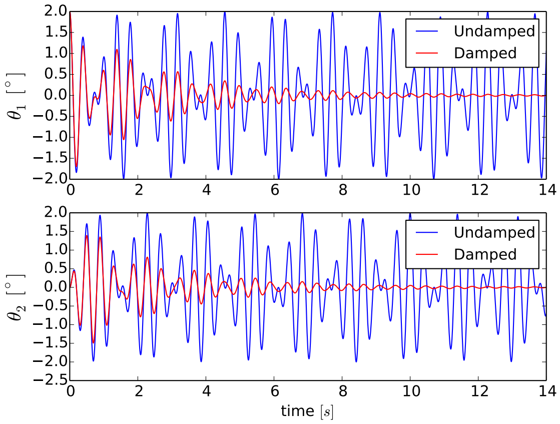

a) Solar panel angles, θ_1 and θ_2.

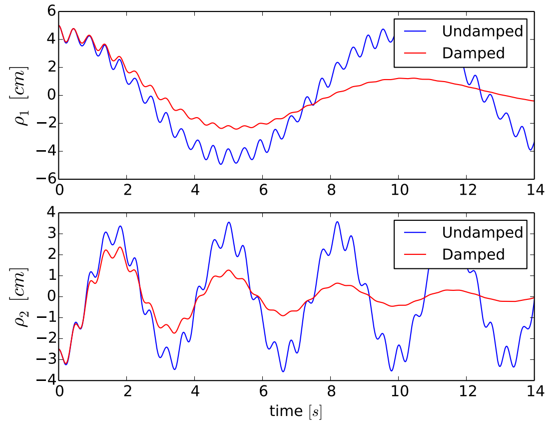

b) Slosh displacements, ρ_1 and ρ_2.

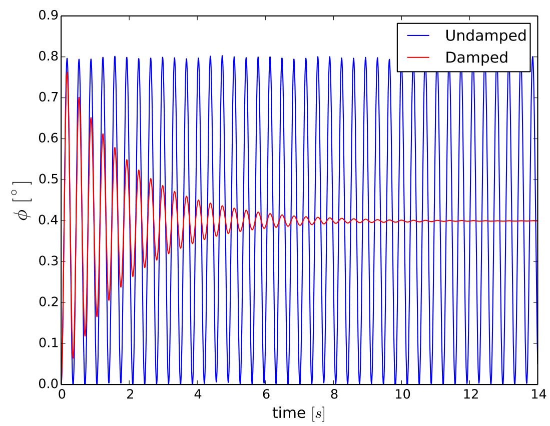

c) Orientation of body frame, ϕ.

Figure 4: Solar panel, slosh, and rotational motion.

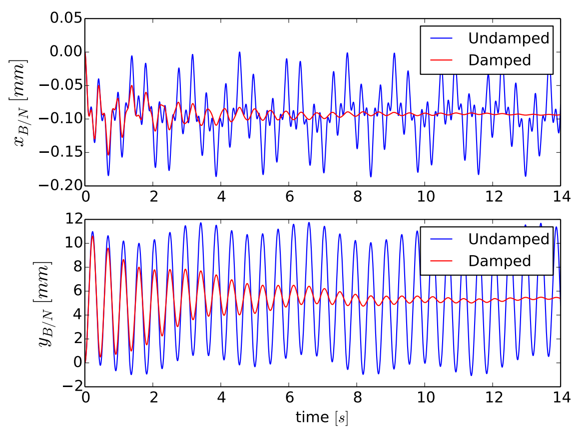

Figure 5: Translational motion of spacecraft.

here that ϕ is only defined for use in this planar case, but otherwise 3-dimensional orientation descriptions would need to be used to describe the relationship between the $\mathcal{B}$ and $\mathcal{N}$ frames. The results from this simulation can be seen in Figures 4-6.

Knowing that total energy needs to be conserved for the undamped case and momentum needs to be conserved for both cases, the results agree with this insight. The first solar panel and both slosh modes initially respond by traveling

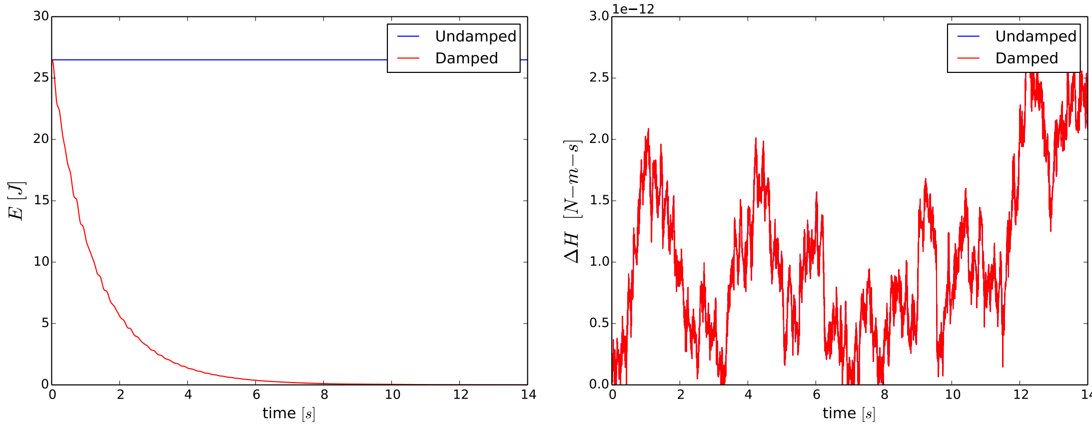

a) Change of total energy of spacecraft. **b)** Variation in the total inertial angular momentum.

Figure 6: Energy and momentum check.

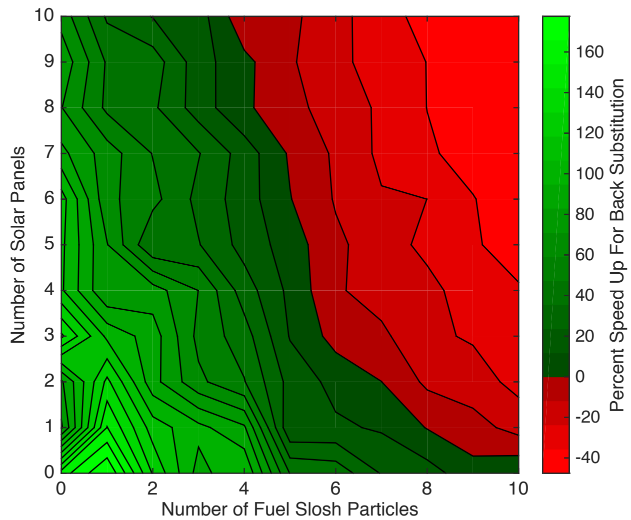

Figure 7: Computational efficiency of back substitution method.

back to equilibrium, and the rotational, translational motions are each affected. Fig. 6 shows that momentum is conserved in both cases, energy is conserved in the undamped case, and energy decays to zero in the damped scenario. This gives confidence in the formulation presented. General three-dimensional motion is also confirmed to obey the laws of physics, and the simple planar case is included for simplicity.

In addition to the numerical simulation, a simple program was developed to quantify the computational efficiency of using the back substitution method. Figure 7 shows the results of this analysis. It is important to note that a Singular Value Decomposition algorithm is used to invert the necessary matrices for this comparison. The percent speed up for the back-substitution method compared to the system mass matrix method is the metric being used. The back substitution performs very well when the number of slosh masses and solar panels are relatively small. 26 percent of the 121 options considered, result in at-least a 50 percent speed up, with 12 of the combinations resulting in over a 100 percent speed up.

However, as expected, as the number of both the slosh masses and solar panels increase, the speed up decreases. With a large number of panels or slosh particles there is still a large matrix to invert which reduces the benefit of the back-substitution method. For large numbers of particles and panels the system mass matrix appears to be more computationally efficient. The reason for the mass-matrix approach being faster is still being investigated. There is a lot of additional math required to perform the back-substitution, which provides additional overhead on top a large sub-component matrix inversion. Depending on the spacecraft and the analysis being completed, the back substitution method can save a significant amount of computation time. For typical spacecraft scenario with 1-3 panels and 3 slosh particles the speed savings is still significant near 50%.

VI Conclusion

A general formulation for incorporating flexible dynamics and fuel slosh into a fully coupled spacecraft simulation is introduced. The flexible and fuel slosh dynamics is approximated using hinged rigid bodies and constraining the lumped fuel slosh particles to travel in a fixed unit direction with respect to the body. Taking in consideration these approximations, this general formulation can apply to a wide range of spacecraft and could be directly applied without the need for re-derivation. Additionally, this paper introduces a back-substitution method to increase computational efficiency.

A numerical simulation is included and energy and momentum behaves appropriately. This validation check gives confidence in the formulation. Furthermore, the back-substitution method can significantly decrease the computational effort and can result in as much as a 180% speedup. For long simulation times, this speedup can be extremely beneficial. However, as the number of slosh masses and solar panels increase the back-substitution method loses its computational efficiency when compared to inverting the system mass matrix. This result will be investigated in the future to understand the reasons for the decrease in computational efficiency and ways to improve the back-substitution method. Additionally, other methods will be investigated to further increase the computational efficiency of the simulation.

The paper acknowledges that there are approximations made, however, for a large population of spacecraft missions, the fidelity of this model is sufficient. Future work will investigate higher fidelity models for both flexing and fuel slosh motion which will give insight into the accuracy of the approximate models.

References

[1] Allard, C., Schaub, H., and Piggott, S., "General Hinged Solar Panel Dynamics Approximating First-Order Spacecraft Flexing," *AAS Guidance and Control Conference*, Breckenridge, CO, Feb. 5–10 2016, Paper No. AAS-16-156.

[2] Sidi, M., *Spacecraft Dynamics and Control: A Practical Engineering Approach*, Cambridge Aerospace Series, Cambridge University Press, 1997.

[3] Angeles, J. and Kecskeméthy, A., *Kinematics and dynamics of multi-body systems*, Vol. 360, Springer, 2014.

[4] Fleischer, G. E. and Likins, P. W., "Attitude dynamics simulation subroutines for systems of hinge-connected rigid bodies," 1974.

[5] Jerkovsky, W., "The structure of multibody dynamics equations," *Journal of Guidance, Control, and Dynamics*, Vol. 1, No. 3, 1978, pp. 173–182.

[6] Zarafshan, P. and Moosavian, S. A. A., "Manipulation control of a space robot with flexible solar panels," *Advanced Intelligent Mechatronics (AIM), 2010 IEEE/ASME International Conference on*, IEEE, 2010, pp. 1099–1104.

[7] Moosavian, S. A. A. and Papadopoulos, E., "Explicit dynamics of space free-flyers with multiple manipulators via SPACEMAPLE," *Advanced robotics*, Vol. 18, No. 2, 2004, pp. 223–244.

[8] Kuang, J., Meehan, P. A., Leung, A., and Tan, S., "Nonlinear dynamics of a satellite with deployable solar panel arrays," *International Journal of Non-Linear Mechanics*, Vol. 39, No. 7, 2004, pp. 1161–1179.

[9] Wallrapp, O. and Wiedemann, S., "Simulation of deployment of a flexible solar array," *Multibody System Dynamics*, Vol. 7, No. 1, 2002, pp. 101–125.

[10] Wie, B., Furumoto, N., Banerjee, A., and Barba, P., "Modeling and simulation of spacecraft solar array deployment," *Journal of Guidance, Control, and Dynamics*, Vol. 9, No. 5, 1986, pp. 593–598.

[11] J., V. and P., V., "Transient and sloshing motions in an unsupported container," *Physics of Fluids in Microgravity*, edited by R. Monti, Taylor and Francis, 1st ed., 2001.

[12] Gerrits, J., *Dynamics of Liquid-Filled Spacecraft*, Ph.D. thesis, University of Groningen, December 2001.

[13] Luppes, R., Helder, J., and Veldman, A., "Liquid Sloshing in Microgravity," *56th International Astronautical Congress of the International Astronautical Federation, the International Academy of Astronautics, and the International Institute of Space Law, International Astronautical Congress (IAF)*, Fukuoka, Japan, 2005.

[14] Abramson, H., "The Dynamic Behavior of Liquids in Moving Containers," Tech. Report SP-106, NASA, 1966.

[15] Dodge, F., "The New Dynamic Behavior of Liquids in Moving Containers," Tech. report, Southwest Research Institute, San Antonio, TX, USA, 2000.

[16] Hung, R. and Chi, Y., "Slosh Dynamics Coupled with Spacecraft Attitude Dynamics Part 1: Formulation and Theory," *Journal of Spacecraft and Rockets*, Vol. 33, No. 4, July-August 1996.

[17] Marsell, B., Gangadharan, S., Chatman, Y., Suddermann, J., Schlee, K., and Ristow, J., "A CFD Approach to Modeling Spacecraft Fuel Slosh," *47th AIAA Aerospace Sciences Meeting Including The New Horizons Forum and Aerospace Exposition*, Orlando, FL, USA, January 2009, Paper No. AIAA 2009-366.

[18] Zhou, R., Vergalla, M., Kirk, D., and Gutierrez, H., "Experimental Methodology and Numerical Technique for 6-DOF Tank Slosh Dynamics," *46th AIAA/ASME/SAE//ASEE Joint Propulsion COnference and Exhibit*, Nashville, TN, USA, July 2010, Paper No. AIAA 2010-6977.

[19] Schlee, K., Gangadharan, S., Ristow, J., Sudermann, J., and Walker, C., "Parameter Estimation of Spacecraft Fuel Slosh," *Structures, Structural Dynamics, and Materials Conference*, Newport, RI, USA, May 2006, Paper No. AIAA 2006-1886.

[20] Theureau, D., Busset, B., Bavestrello, H., Dandaleix, L., Tanguy, S., Mignot, J., and Maureau, J., "Integration of low g sloshing models with spacecraft attitude control simulators," *AIAA Guidance, Navigation, and Control (GNC) Conference*, Boston, MA, USA, August 2013.

[21] Buseck, R. and Benaroya, H., "Mechanical Models for Slosh and Liquid Fuel," *Aerospace Design Conference*, Irving, CA, USA, 1993, Paper No. AIAA-93-1093.

[22] Enright, P. and Wong, E., "Propellant Slosh Models for the Cassini Spacecraft," *Astrodynamics Conference, Guidance, Navigation, and Control*, Scottsdale, AZ, USA, 1994, Paper No. AIAA-94-3730-CP.

[23] Kana, D., "A Model for Nonlinear Rotary Slosh in Propellant Tanks," *27th Structures, Structural Dynamics and Materials Conference Structures, Structural Dynamics, and Materials*, San Antonio, TX, USA, 1986.

[24] Schaub, H. and Junkins, J. L., *Analytical Mechanics of Space Systems*, AIAA Education Series, Reston, VA, 3rd ed., 2014, doi:10.2514/4.102400.